4. Paleoclimate and Climate Dynamics

4.1. Introduction

The study of paleoclimate can be profoundly compelling, perhaps because we are uncovering the circumstances of our origins. An investigation of the paleoclimate record and causes of observed variations helps us to understand how the climate system works. The field of *climate dynamics* uses the laws of physics to try to understand the mechanisms of climate change and apply them in the past, present, and future. Since climate change has influenced humans in the past, anthropogenic climate change will also affect us.

Climate has helped shape the course of civilization. Consider the *Medieval Optimum* during ~900-1400 AD, when the extratropical Northern Hemisphere was 1-1.5 K warmer than during the *Little Ice Age* that followed (~1400-1890 AD). During the Medieval Optimum, a prolonged warm period in the Southwestern U.S. fostered the blossoming of the Anasazi culture. The Anasazi succumbed to a particularly prolonged drought around 1130 AD. Tree ring data will be shown which supports the idea that the population growth outstripped the local carrying capacity of the land during a drought [Diamond, 2005]. The Medieval Optimum also coincided with the Viking occupation of Greenland during 970-1400, who ceased habitation there at the beginning of the Little Ice Age. Large volcanic eruptions, or clusters of eruptions, have been repeatedly linked with colder summers and crop failures, together with warmer and wetter winters in Eastern North America and Eurasia.

Salient paleoclimate events will be described which motivate discussion of possible climate dynamical explanations. One powerful approach in trying to understand climate dynamics is *determinism*. As Richard Feynman described it, "All one has to do is know the initial conditions and the laws of physics, and then the evolution is determined" [Gleick 1990]. Determinism attempts to distinguish cause from effect and to work out specific lines of reasoning. The technological achievement of humans walking on the moon is testimony to the success of deterministic reasoning. However, the complex interaction among the parts of a system can yield unexpected results, and one cannot know the state of a system to an arbitrarily precise degree. These factors imply significant limitations on how well we can predict the system's evolution. These ideas underlie the relatively recent field of *chaos theory*, pioneered by atmospheric scientist Ed Lorenz in 1961. Chaos theory recognizes that the natural world contains inherent unpredictability, that is, it's chaotic, and that even a simple system such as a water wheel is hopelessly unpredictable [Gleick 1990].

One compelling mystery is how the earth goes into ice ages and back into interglacial times, such as the one we are in now (the *Holocene interglacial*). The *Milankovich theory* of climate change is fundamentally deterministic, but is compatible with chaos theory, and the climate system exhibits elements of both. Another intriguing puzzle is the cause of strong temperature oscillations (~10-20 K) during glacial times. These temperature variations at millennial time scales may be linked to variations in the formation of deep water in the North Atlantic and Antarctic. Millennial oscillations have also been observed in the Holocene, but were only ~2 K in magnitude. Millennial oscillations are related to variations in the strength of the *Atlantic Meridional Overturning Circulation* (AMOC). The effects of volcanic eruptions are also investigated, which can have influences over a broad range of time scales.

4.2. Evidence of Past Change

Many inventive techniques from a variety of perspectives contribute to our understanding of what happened in the past. Sources of information include bore hole temperature data, corals and other fauna, pollen, ice cores, lake levels, isotopic and chemical methods, speleothems, lichens, periglacial features, and tree rings. You may download and plot paleoclimate data from http://www.ncdc.noaa.gov/paleo for your own investigations. (Just be sure to give proper citation to the data source.)

Interpretation of tree rings (*dendrochronology*) provides an absolute time scale, often accurate to the year, for an event in the distant past, hundreds or even thousands of years ago. Warm rainy years foster large growth rings and small growth rings are indicators of drought. A unique tree ring pattern for a given region can be constructed by finding live, dead, and fossil tree trunks that overlap and are successively older in age. One sequence of oak has been extended back 10,000 years. Some fossil tree sequences go back to 40 kybp. Dendochronology sequences are useful for calibrating *radiocarbon dates*. They can even be used to show the geographical pattern of summertime cooling after major eruptions [Briffa et al., 1998].

Lichens provide another interesting means of dating objects. They are symbiotic combinations of algae and fungi, somewhat analogous to the fungal mycorrhizae / root hair association for trees and the coral symbiosis with algal zooxanthellae. Lichens festoon trees in damp environs and form thick carpets in the boreal forest and tundra for the caribou to eat. Lichens help cleanse the environment of pollutants, but are especially sensitive to acid rain. As an infusion in tea, *usnea*, or Old Man's Beard, is said to be helpful with lung ailments, as well as being part of the "lungs of the planet" [Buhner, 1996]. The growth rate of each lichen species helps us relate their size to their age. Their size on boulders is useful for dating the retreat of glaciers.

Since vegetation type is closely linked to climate, information about the mix of plants and how they varied with time can be quite revealing. A handy recording mechanism is provided by the annual signal in lake sediments. During snowmelt in the spring, or after the rainy season, high flow washes pollen from a drainage basin into a lake, where it settles into the bottom, leaving annual layers, or *varves*. To cite a famous example, the Dryas flower favors cold climates. During the Younger Dryas event (12.9 - 11.6 kybp), pollen from this flower was found over a much wider area of northern Europe than during the subsequent Holocene and the preceding Bolling/Allerod warm period. Annual pollen sequences from Lake Van in eastern Amatolia go back ~ 600,000 years and show a rise in pine and oak pollen near Gobekli Tepe at the end of the Younger Dryas (Pickarski et al. 2015).

Fossil animals and plants are also useful in determining paleoclimate. Subarctic islands bear fossils of alligator and palm tree species from the Cretaceous. Certain radiolarians, a type of phytoplankton, have a threshold temperature which determines the direction in which they coil, right or left. By examining a deep-sea sediment core, one may determine when the sea surface water was above or below this temperature threshold. Since corals can grow only in the temperature range ~24-30°C, the record of fossil corals, in conjunction with chemical dating techniques, informs us of paleoclimate in the world's tropical oceans.

Focus: Radiocarbon dating

^{12}C has 6 electrons, 6 protons and 6 neutrons, while ^{14}C has 2 extra neutrons. ^{14}C is created when cosmic rays from outer space strike a nitrogen molecule in the atmosphere. ^{14}N has 7 electrons, 7 protons, and 7 neutrons. But when a cosmic ray strikes it, one proton can be converted to a neutron, making ^{14}C. There is a distinct variation in the amount of cosmic rays reaching earth on quasi-millenial time scales, and this signal must be accounted for in estimating age with the ^{14}C technique. A live organism either photosynthesizes ^{14}C or eats the plants that has fresh ^{14}C. If it is buried when it dies and stops exchanging gases with the atmosphere, then the ^{14}C starts decaying to ^{12}C at an inexorable, predetermined rate.

For land samples with organic material emplaced less than 40,000 years ago, one may tell its age by analyzing the amount of ^{14}C relative to ^{12}C. ^{14}C is radioactively unstable and decays with a half-life of 5370 years. It is hard to predict when a single ^{14}C nucleus will spontaneously emit 2 neutrons and decay to ^{12}C, but with a sample containing enough carbon molecules, the decay follows a precise exponential shape. The original amount of ^{14}C will decay to 1/2 of its original value in 5370 yr, to 1/4 at 10,740 yr and to 1/8 at 21,480 yr and to 1/16 at 42,960 yr. After that, the amounts of ^{14}C are so small that the uncertainty in time becomes too large. Material in sediments sequestered for a long time contains a low fraction of ^{14}C.

The action of waves on the shore can scoop material away, making for shelf-like structures. When ice builds up on land during an ice age there is less water in the ocean, so sea level falls. As sea level falls, shelves are made at lower and lower levels on the shoreline. Submerged shelf-like shorelines are evidence of melting glaciers and rising sea levels. Since the *Wisconsin Ice Age*, sea level has risen ~ 120 m in ~ 20,000 yr, an average of 6 m per 1000 yr. In the last 6,000 years, sea level has been quite stable, rising less than 3 m.

Regional changes in sea level can occur through *isostatic rebound*. Once large land glaciers melt, the ice no longer weighs down the crust. By Archimedes' buoyancy principle, the elastic asthenosphere will help push the unburdened crust upward. Rebound of the Gulf of Bothnia has closed the valleys formed by eastward-flowing ice-age mountain glaciers in northern Sweden and made them into long lakes. The rate of isostatic rebound at different parts of the world can be measured and extrapolated backward into the past to help quantify the mass of glacial overburden.

During cold times moving glaciers can transport rocks and dirt. Lateral and terminal moraines tell us about the advance and retreat of glaciers. Continental glaciers exhibit a slow plastic movement, with downward flow in the snow accumulation zone in the center, then flowing out to the sides. At the bottom a glacier can pluck rocks from the substratum and carry them long distances to the edge of the continent. Calving ice bearing these rocks can float out to sea, where they eventually melt, letting the rock debris sink to the bottom of the ocean and become incorporated into the sediment record. Periods of ice-rafted rock debris from the central Canadian shield of pre-Cambrian pink granite can be found in deep sea cores throughout the North Atlantic. Periods of rapid warming in a glacial state can generate large amounts of ice-rafted rock debris. These have come to be called *Heinrich events*.

Cold times also favor the transportation of windblown, or aolean, dust. Central Asia is far from the oceans. During the Ice Ages, not much snow fell on northern Siberia and the ice masses were small compared with the Laurentide ice sheet, which grew thick with snow from the moisture source over the nearby Atlantic Ocean. Central Asia became very cold and dry. Winds easily picked up sand and dust from the dry desert steppes across Asia and spread it around the world, being notable in Pacific deep sea sediment records. This type of dust reflects sunlight and cools the planet, constituting a positive feedback in the climate system. Similarly, during warm times the lack of dust allows further warming. Aolean dust also plays a major role in providing mineral nutrients for the growth of phytoplankton and plants on islands far from continents.

4.3. The Paleoclimate Record

Paleoclimate phenomena and corresponding time scales of interest include

- the *faint young sun paradox* (billions of years),
- periodic extinctions and the *Oort cloud* (27 million-year periodicity),
- the *Cretaceous warm period* (145-65 Mybp),
- Antarctic continental drift (10 Mybp),
- glacial /interglacial cycles (last million years),
- the *Eemian interglacial* (130-115 kybp),
- *Wisconsin glacial maximum* (20 kybp),
- the *Bolling/Allerod* warm period (14.6-12.9 kybp)
- the *Younger Dryas* cold event (12.9-11.6 kybp),
- Heinrich and *Dansgaard-Oeschger events* (millennial cycles),
- the *Holocene maximum* (2-8 kybp),
- the *Medieval Optimum* (600-1100 ypb; 900-1400 A.D.),
- and the *Little Ice Age* (130-620 ybp; 1400-1890 A.D.)

Factors to be examined in accounting for these events include the sun, asteroids, plate tectonics, the Milankovich theory of orbital parameters, ice albedo, vegetation, and greenhouse gas feedbacks, the thermohaline circulation, volcanism, and chaos theory. (The Dust Bowl Years (1930s), and the End-of-Millennium Warming will be discussed in Chapter 7.)

4.3.1. The faint young sun paradox

Astronomy informs us that our sun is a member of a group of similar stars which can be observed at different stages of their life cycles. Our sun was likely to have been rather variable in its output during the first few 100 M years, with more intense outflow blowing the early atmospheres of the inner planets into outer space. The atmospheres that developed later were gradually outgassed from liquid interiors. On earth this was primarily water vapor and carbon dioxide. Within 1 B years, the sun equilibrated to a solar output that was ~75% of its current output. Taking 0.75 S in (2.7) with A=0.3 gives T_{re} = 202 K, which is far below the freezing point of water.

You may wonder whether the earth was ever entirely covered by ice. Why wouldn't it be, if the solar output was weaker? Evidence does not support a sustained "ice-ball earth". The most likely explanation is that there was much more CO_2 in the atmosphere, perhaps 20-30 times as much, with the strong greenhouse effect compensating for the faint young sun. If this is the case, then there has been a serendipitous, gradual decline in atmospheric greenhouse constituents over geologic time which has roughly compensated for the gradually-strengthening solar output. James Lovelock argued that life on earth is responsible for this homeostasis through photosynthesis and other processes, the *Gaia hypothesis*.

The rise of biodiversity has been punctuated by abrupt, cataclysmic species loss, demarcating the end of major geological periods and the beginning of new ones (Fig. 1.7). It is believed that most of these are caused by impacts of objects from outer space. Whether they are comets or asteroids or large meteors, these bolide impacts have had a tremendous influence on our planet and will in the future. The impact which resulted in the end of the Cretaceous period and beginning of the Tertiary period at 65 Mybp, the "KT boundary", occurred near the northern tip of the Yucatan peninsula. Numerical simulations suggest that this extremely energetic impact ejected vast sheets of incandescent, molten earth over forests, catching them on fire, choking the atmosphere with a debris cloud that shut off sunlight and photosynthesis, so that many forms of life became extinct.   Mammals had been outcompeting the dwindling dinosaurs for millions of years, and this was the final nail in their coffin.

4.3.2. The Oort cloud and species extinction

One rather uncomfortable theory is that there is something about the way the solar system goes through space that yields periodic extinctions every 27 M yr. The idea is that every 27 M yr our solar system passes near something that gravitationally perturbs the numerous but distant cloud of objects, called the Oort cloud. These objects slowly orbit the sun far beyond Pluto. At these times, objects are perturbed, fall toward the sun, and have a greater likelihood of hitting the earth and causing abrupt climate change and species loss.

One implication of these massive impacts is that rocks from earth have been ejected to the moon, Mars, and Venus, and vice-versa. It is likely that rocks containing life spores have been spread through our solar system by this process. It would be interesting to dig up the regolith of the moon, which contains 10% material which is not originally from the moon, to try to better understand the evolution of our solar system and of life on earth.

4.3.3. Cretaceous warm period

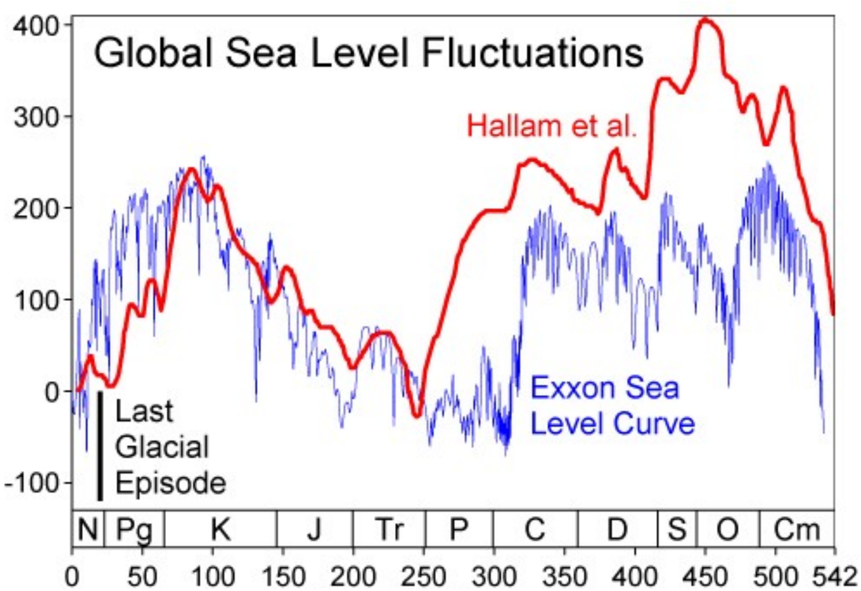

Figure 4.1. Variations in sea level (meters) over the past 500 million years [IPCC 2007].

Over 100s of millions of years the earth moved gradually into and out of warmer and colder periods, with associated sea level rise and fall. Figure 4.1 shows that sea level reached peaks several times during 500 - 300 Mybp, and then reaching another broad peak during the Cretaceous (150-65 Mybp).   The 120 m lower sea level 20,000 ybp is shown for comparison. It is believed that the speed of convective overturning in the earth's mantle varies at these time scales. When overturning is faster, oceanic plates are subducted under continental plates more vigorously, with more volcanic emission of CO_2. This would favor melting of land glaciers and thermal expansion of the ocean. The rate of overturning may also change the depth profile of ocean basins, with more rapid mantle overturning causing higher sea levels. Exchange of water between the ocean and the mantle can also cause the ocean volume to change over time. The Cretaceous sea level maximum was likely 100 m ±50 m higher than present, with temperature changes at 10-100 My time scales, attributed to tectonically-controlled carbon dioxide variations [Miller et al. 2009].

During the Cretaceous (65 - 150 Mybp) the global mean temperature was at least 10 K warmer and sea level was at least 100 m higher. It is likely that there was more than 10 times as much CO_2 in the atmosphere as at present. "Cool-blooded" dinosaurs roamed the earth. The Arctic was inhabited by plants and animals normally associated with warm climates.

Another very warm episode occurred during the early Eocene, about 55-50 Mybp. This period is of interest because it may have been similar to what might occur in the next 100 years, with acidification of the ocean and drastic shifts in oceanic species composition. This warm period gradually gave way to cooling, as Antarctica gradually drifted toward the South Pole over the past 25 M yr. For the past 2-3 M yr, in its position over the South Pole, Antarctica has anchored the climate in an ice house period, by acting as a giant solar reflector and infrared emitter: the planetary refrigerator.

4.3.4. Glacial / interglacial cycles

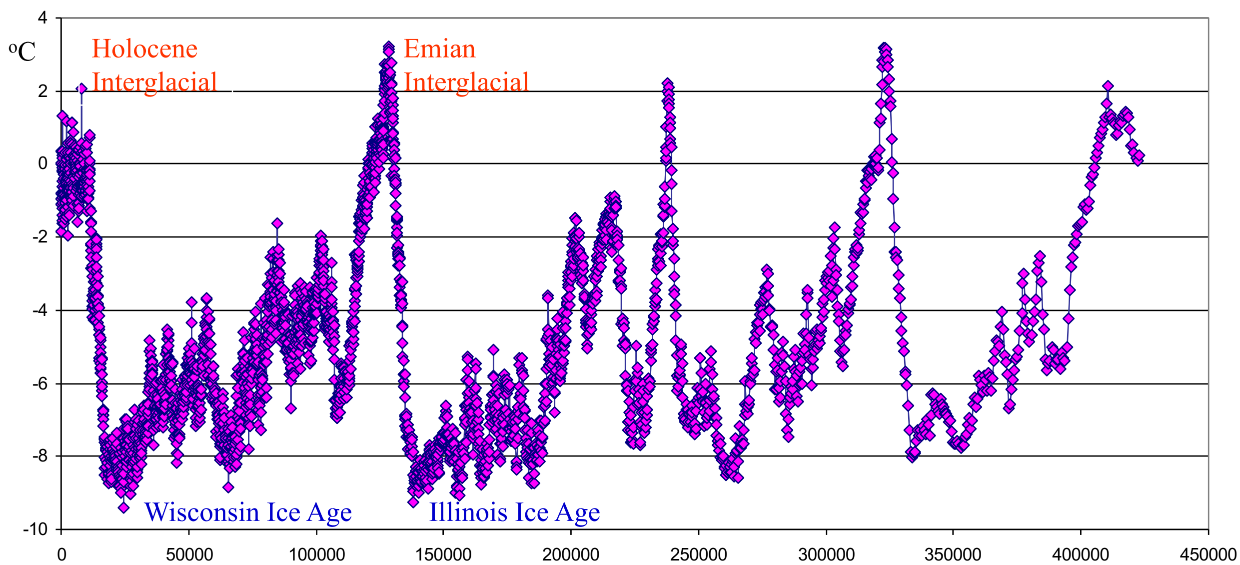

Figure 4.2. Global temperature variations over the last four glacial / interglacial cycles inferred from Vostok deuterium [Petit et al. 2001; data from www.ncdc.noaa.gov/paleo].

During the past million years, there have been about 7 major cycles of glacial and interglacial times. Figure 4.2 shows the last four glacial / interglacial cycles seen in the 420,000 years Vostok ice core record. Temperatures were derived from deuterium isotope variations and are representative of the extratropical Southern Hemisphere. Periodicities near ~100,000 yr, ~41,000 yr, and ~23,000 yr are discernable in this record [Petit et al. 2001]. Note that cooling progresses irregularly over long time periods, while warming can occur quite rapidly. The

Laurentide Ice Sheet advanced out of Canada all the way to Illinois 170 kybp and to Southern Wisconsin 20 kybp. To find times warmer than the present, one would have to return to the Emian interglacial of 130-115 kybp, when half of the Greenland ice sheet was melted and sea level was ~6 m higher. The CO_2 concentration during the Emian never exceeded 300 ppmv (Fig. 1.2). It seems likely that, by doubling or tripling CO_2 in this century, there will be significant melting of Greenland. We will return to this topic in Chapter 7.

The last 100,000 years have been characterized by a variable, but downward trend in temperature toward the Wisconsin Ice Age maximum 20 kybp (Fig. 4.2). The descent toward a glacial state typically occurs in a series of sawtooth declines with periodicities near 22,000 and 41,000 years, while warming to an interglacial state occurs comparatively quickly. This provides clues for distentangling the various feedbacks within the system. An especially cold time along the way occurred about 70 kybp (Fig. 4.2), coinciding with the eruption of Mt. Toba in Sumatra, which left a lake 70 km wide. During the last 100,000 years Neanderthals spread throughout Africa and Eurasia, with commingling Cro-Magnons beginning ~40 kybp. Whether they were truly distinct species we may never know, but by 40 kybp humans were creating art preserved in caves that strikes us as pleasingly adept.

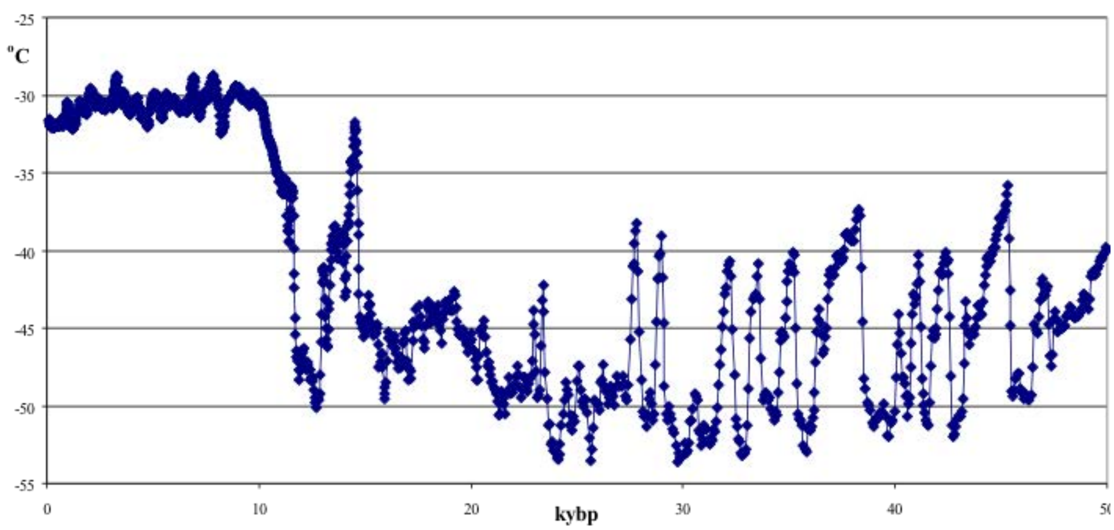

Figure 4.3. Variations in Greenland surface temperature (°C) at GISP2 over the past 50,000 years. Note the common occurrence of Dansgaard-Oeschger events during the Wisconsin Ice Age, but not during the Holocene [Alley et al. 2000, 2004, www.ncdc.noaa.gov/paleo].

Figure 4.3 shows variations in Greenland surface temperature at GISP2 (72°N, 38°W) over the past 50,000 years. The top of the GISP2 core is at 3200 m altitude and its bottom is 3053.44 m deep, spanning some 130,000 years. Note the striking temperature swings that were common throughout the Wisconsin Ice Age, on time scales of hundreds to thousands of years. These Dansgaard-Oeschger events were much weaker during the Holocene, when the Laurentide Ice Sheet was minimal or absent. The most recent temperature spike was the Bolling/Allerod period (14.6-12.9 kybp), which was followed by the Younger Dryas event. It was named after the white Dryas flower which is normally confined to the Arctic, but grew plentifully across northern Europe at this time. We will return to the Younger Dryas event when discussing the North Atlantic oscillator theory of climate change.

The temperature trend emerging from the Wisconsin Ice Age was somewhat different at Greenland and Antarctica. Figure 4.4 shows variation in deuterium, temperature, ^{18}O, CO_2, and CH_4 at Vostok over the past 25,000 years. Over Antarctica, temperatures were constant and cold during 25 - 17 kybp, with a ramp up to a constant and warm period after 11 kybp (Fig. 4.4b). The Bolling/Allerod and Younger Dryas events are considerably damped-out relative to the signal at Greenland (Fig. 4.3). The estimated temperature record (Fig. 4.4b) differs slightly from the deuterium record (Fig. 4.4a), due to corrections for variation in global ice volume and temperature of the deep ocean. The variation in ^{18}O (Fig. 4.4c) at Vostok is not identical to that of deuterium, because of differences in the budgets for different earth system reservoirs.

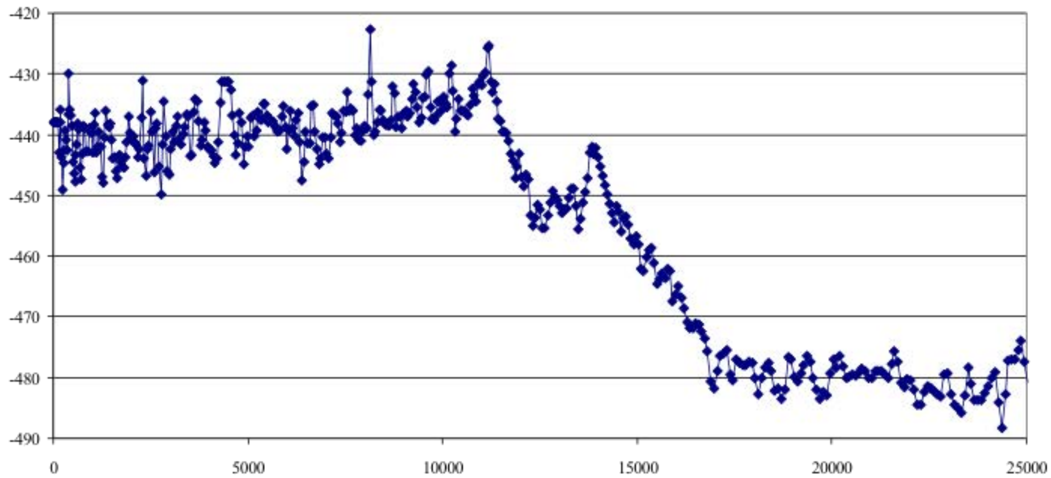

Figure 4.4a. Variation of deuterium (ppt departure from ocean mean) at Vostok, Antarctica over the past 25,000 years [Petit et al. 2001; data from www.ncdc.noaa.gov/paleo].

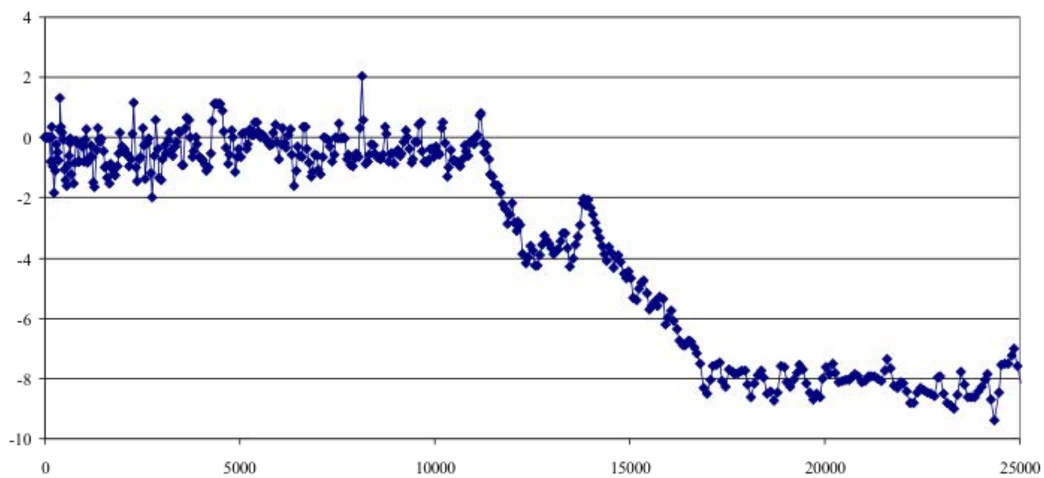

Figure 4.4b. Variation of global temperature over the past 25,000 years estimated from Vostok deuterium [Petit et al. 2001; data from www.ncdc.noaa.gov/paleo].

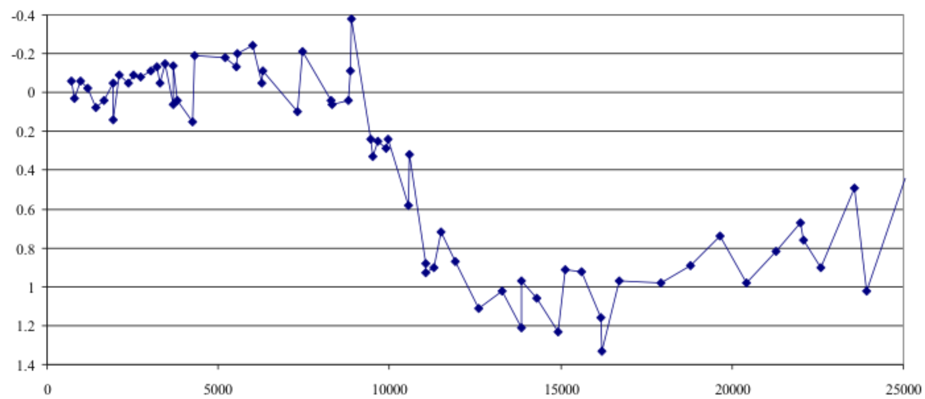

Figure 4.4c. Variation of ^{18}O (ppt departure from ocean mean) at Vostok, Antarctica over the past 25,000 years [Petit et al. 2001; data from www.ncdc.noaa.gov/paleo].

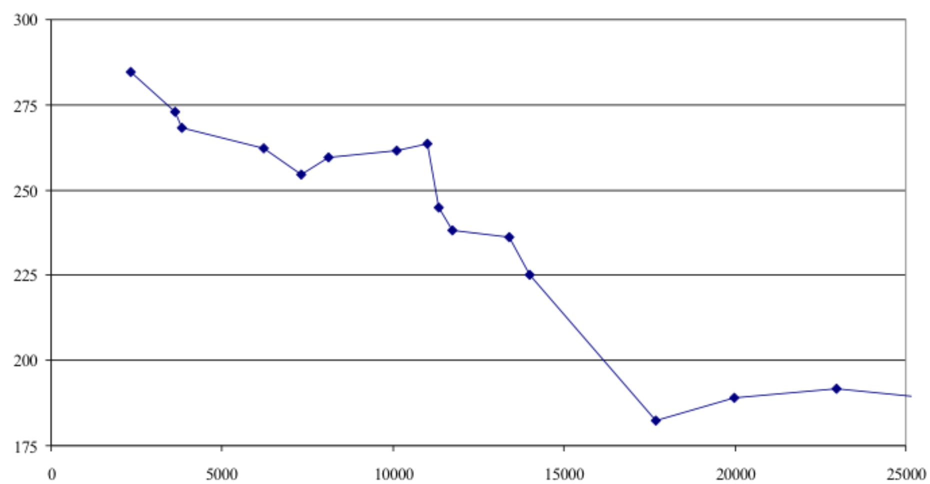

Figure 4.4d. Variation of CO_2 (ppmv) at Vostok, Antarctica over the past 25,000 years [Petit et al. 2001; data from www.ncdc.noaa.gov/paleo].

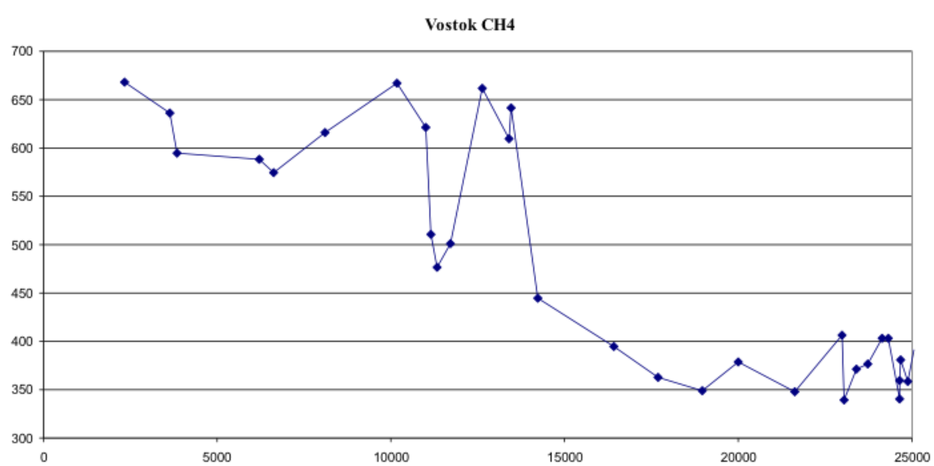

Figure 4.4e. Variation of CH_4 (ppbv) at Vostok, Antarctica over the past 25,000 years [Petit et al. 2001; data from www.ncdc.noaa.gov/paleo].

Variations of CO_2 (Fig. 4.4d) are similar to variations in temperature. The basic features of the signal in methane (Fig. 4.4e) are similar, but methane is much more responsive to shorter time scale changes, such as the Bolling/Allerod and Younger Dryas events. This type of information regarding the timing of greenhouse gas trends is useful in helping us to understand how the earth system might evolve over the next few hundred years.

Figure 4.5 shows the variation in Greenland surface temperature during the transition from the Wisconsin glacial maximum to the Holocene, emphasizing the Bolling/Allerod and the Younger Dryas events. The warmings exceeding 10 K near 14.6 kybp and 11.6 kybp were quite rapid, with step-function increases in the rate of snow deposition occurring in just a few years [Alley et al. 1993]. It is interesting that the abrupt doubling of accumulating snow requires a warming of 7 K according to (3.1), which governs the saturation vapor pressure dependence on temperature. This is consistent with temperature changes seen in Fig. 4.5. The associated rapid melting of the Laurentide Ice Sheet is termed a "*hosing event*" in climate modeling. The injection of fresh water into the North Atlantic surface waters affects the thermohaline circulation and can lead to temperature changes hundreds to a few thousand years later.

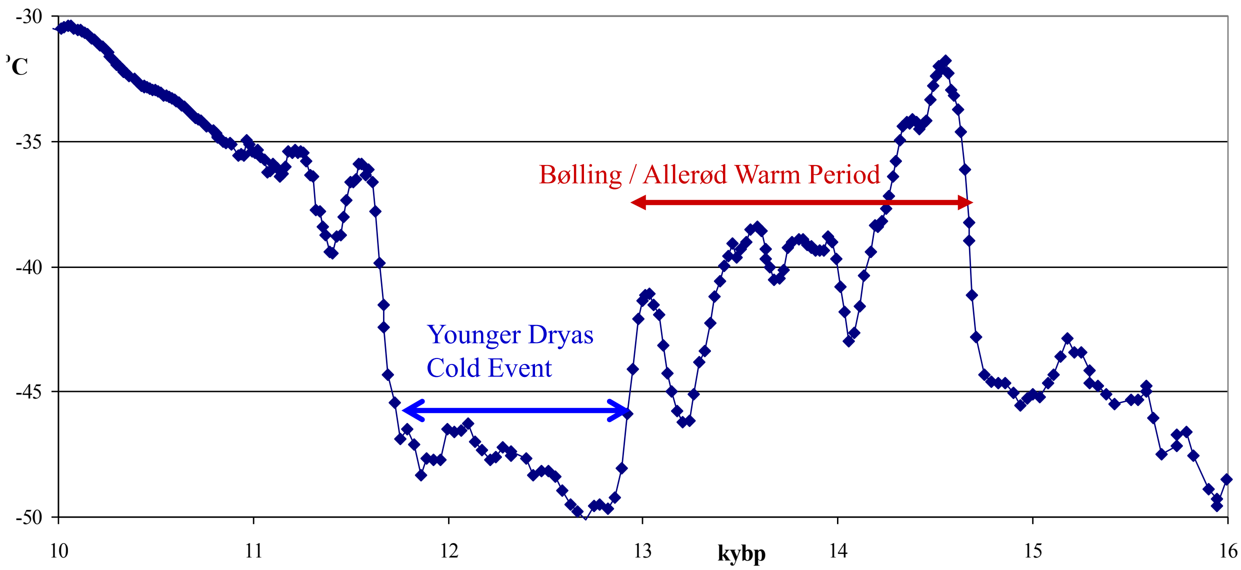

Figure 4.5. Variation in Greenland surface temperature during 16 – 10 kybp [Alley et al. 2000, 2004, www.ncdc.noaa.gov/paleo]. The Bølling / Allerød period (14.6 – 12.9 kybp) began with, and the Younger Dryas period (12.9 - 11.6 kybp) ended with rapid warming.

A prolonged meltwater pulse from Antarctica ("meltwater pulse 1a") ~ 14-15 kypb led to increased North Atlantic bottom water formation (Weaver et al., 2003). This coincided with an increased heat flux to the northern high latitude atmosphere, ushering in the Bolling / Allerod warrm period seen in Greenland (Broecker, 1998). At the Wisconsin glacial maximum, sea water was stored in the form of compacted snow on land surfaces, primarily in North America and northern Eurasia. Figure 4.6 shows radiocarbon isochrones (see focus on ^{14}C) of the retreat of the Laurentide Ice Sheet. Times of rapid melting of the Laurentide Ice Sheet coincided with surges of glacial material from Hudson Bay out the Davis Strait into the Atlantic Ocean (Fig. 4.7), causing Heinrich events of ice-rafted rock debris.

Figure 4.9a shows the change in sea level from 22 kybp to the present. Note the meltwater pulse near 14.6 kybp that ushered in the Bolling / Allerod period. The ice edge retreated northward past the St. Lawrence river between 12 and 11 kybp (Fig. 4.6), consistent with the rapid temperature increase in Greenland at the end of the Younger Dryas (Fig. 4.5). This allowed meltwater from the Laurentide Ice Sheet to flow out the St. Lawrence River to the Atlantic ocean. When Stonehenge and the Egyptian pyramids were being built about 5000 years ago there was still significant ice remaining in Labrador and west of Hudson Bay (Fig. 4.6).

Figure 4.6. Radiocarbon isochrones of the retreat of the Laurentide Ice Sheet [Reid Bryson, personal communication].

Figure 4.7. Bathymetry of the North Atlantic region [http://www.gebco.net/].

Sometime during this last ice age humans made their way from Asia to North America via the exposed land bridge of Beringia (Fig. 4.8). Some probably made their way down the west coast in primitive boats, while others made their way into the interior east of the Cordilleran Ice sheet, which was anchored in the Canadian Rockies. By 14 kybp a distinctive stone point making culture, the Clovis people, was found all throughout the Americas. By 12 kybp all of the megafauna were hunted to extinction, including the Giant Deer, Woolly Mammoth, and the Cave Bear. Some trees that have remained as relict partners with these "charismatic megafauna" include the anomalously large-fruited Osage-orange and catalpa trees. The last Woolly Mammoth lived on Wrangell Island, northeast of Siberia, until about 3 kybp. It was a smallish variety. Perhaps the smaller ones were able to survive on the more limited food of the island, away from people.

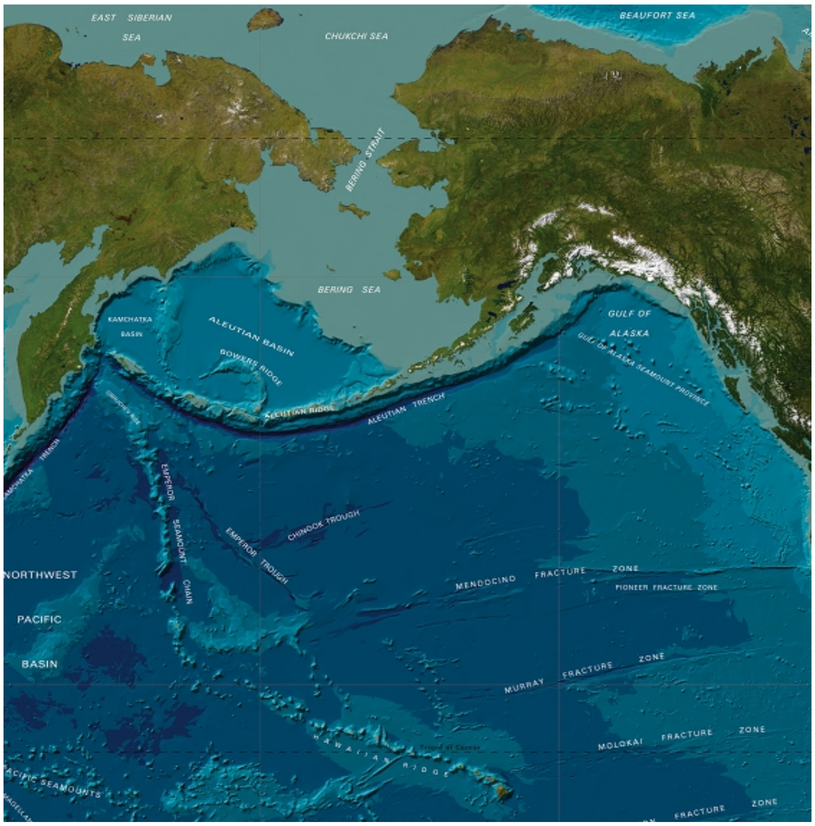

Figure 4.8. The Bering Sea between Alaska and Russia is less 200 m deep (lightest gray). During the Wisconsin Ice Age sea level was 120 m lower than at present, exposing a land bridge to central Alaska and a route southeastward along the coast [www.gebco.net/].

4.3.5. The Holocene

Figure 4.9b shows the changes in sea level over the past 10,000 years (the Holocene). The melting of North American and Eurasian ice sheets caused sea level to rise until stabilizing around 6,000 years ago. Around 7.5 kybp the rising Mediterranean flooded through the Bosporus and over a waterfall, causing the waters of the Black Sea to rise. A previously submerged shoreline at about 100 m depth dotted with ancient villages dates from this time. This event may have been the basis for the oral tradition of a great flood which was prevalent among ancient tribes in the Middle east [Ryan and Pitman 1998].

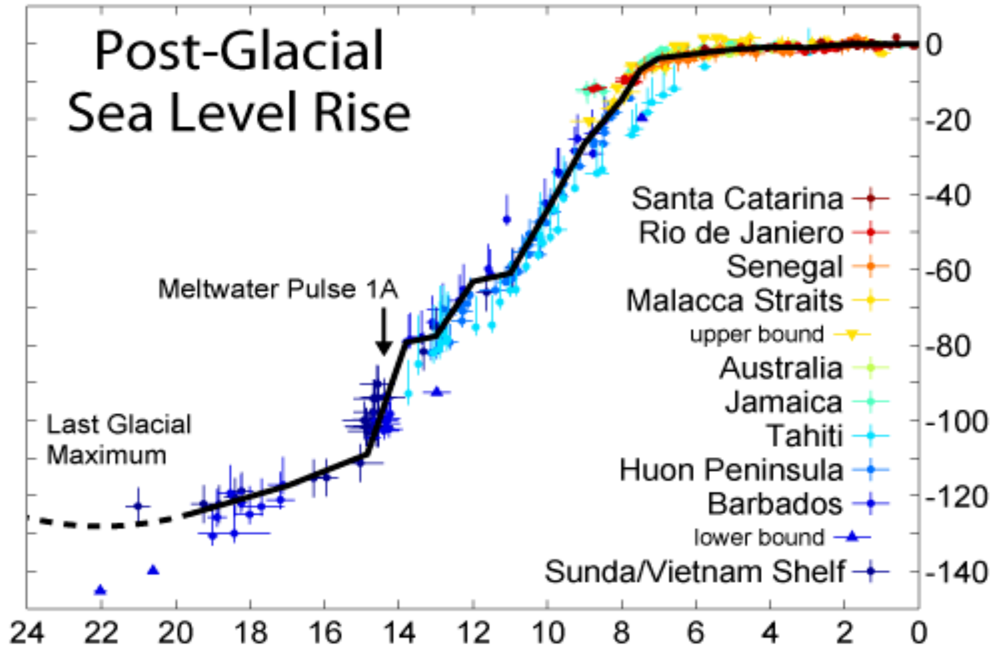

Figure 4.9a. Change in sea level (meters) from 22 kybp to the present. Note the meltwater pulse near 14.5 kybp that ushered in the Bølling / Allerød period [IPCC 2007].

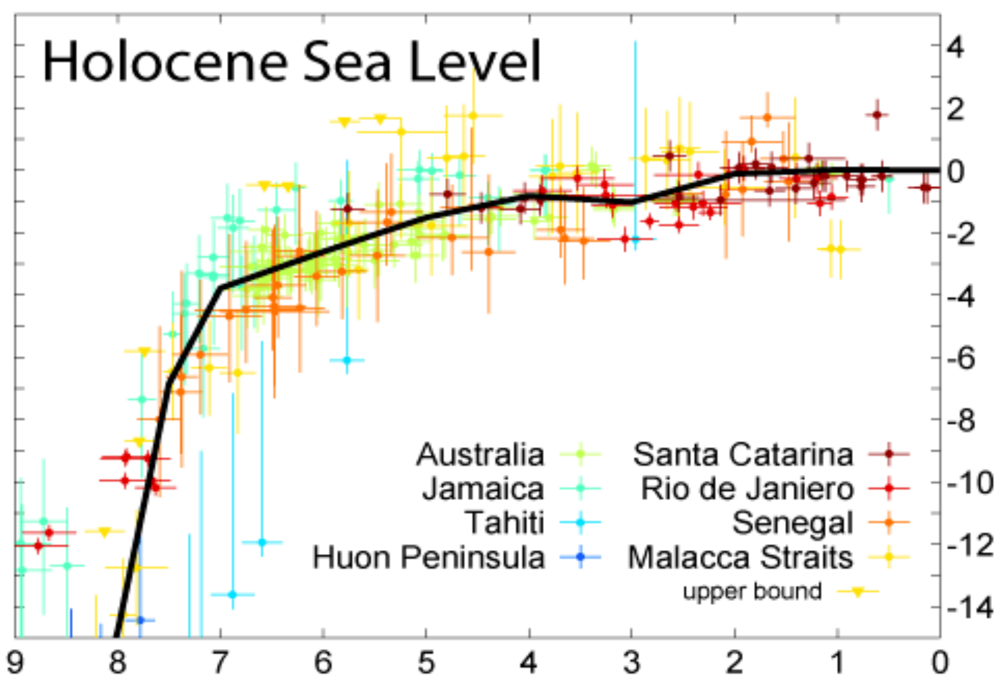

Figure 4.9b. Change in sea level (meters) from 8 kybp to the present. Note the stability of sea level during the rise of civilization [IPCC 2007].

By 8 kybp, the earth was getting warm enough to favor the rise of large-scale farming across both the Old and New Worlds. Ruddiman (2003, 2007) proposed that anthropogenic climate change began more than 6000 years ago. This *Early Anthropogenic Hypothesis* suggests that widespread deforestation and the emergence of agriculture led to a gradual but significant rise in atmospheric CO_2 and CH_4. This may explain the unusual length of the Holocene maximum relative to previous interglacials. If this is true, then humans have been unwittingly *geoengineering* the planet's temperature for the duration of civilization. This suggests that we are already engaged in keeping the planet from going into an ice age. It renders the question "Should we consciously geoengineer now?" somewhat more palatable. We will return to this topic in Chapter 12.

The stability of sea level during the Holocene is likely to have been a major factor in the rise of civilization. A stable sea level generates complex tidal estuaries and shoreline features that provides important food sources. It is consistent with reduced climate variability and greater reliability of food sources.

How much did the climate vary during the Holocene? Figure 4.10 shows the variation in Greenland temperature over the past 10,000 years. Variations of the order 2-3 K are evident, with a fascinating quasi-millennial periodicity. These significant temperature variations exerted important influences on various cultures during the Holocene [e.g., Bryson and Bryson 1997]. The cause of these millennial variations, which includes the Medieval Optimum and the Little Ice Age, remains elusive. Perhaps it represents a natural chaotic mode of the climate system, or it may be related to extraterrestrial periodicities.

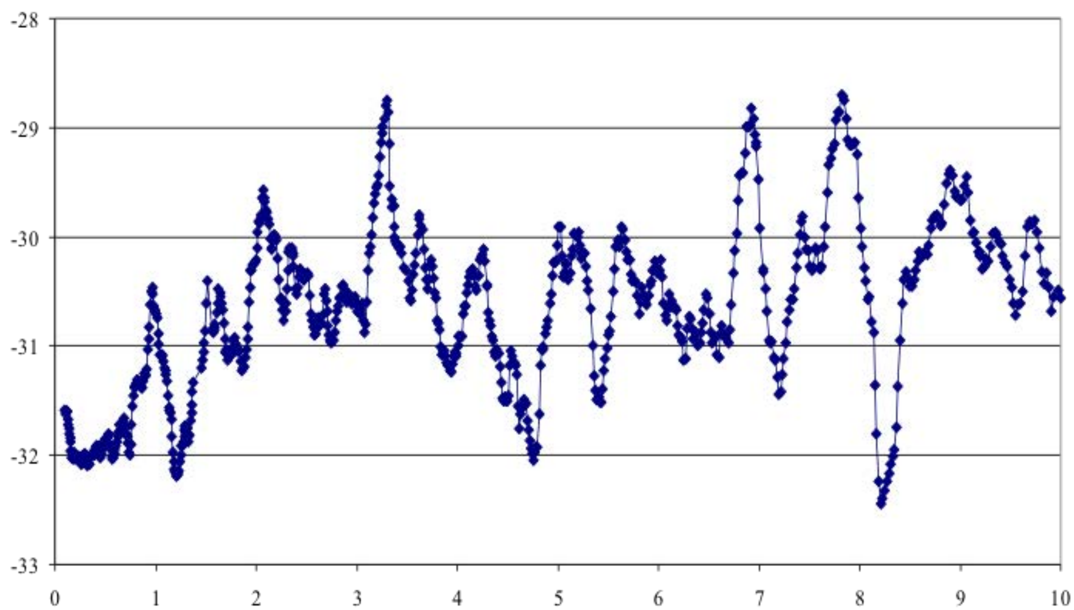

Figure 4.10. Variations in Greenland surface temperature (°C) at GISP2 over the past 10,000 years. Note the interesting variability at millennial time scales [Alley et al. 2000, 2004, www.ncdc.noaa.gov/paleo].

A strong candidate explanation is that millennial variations are related to the strengthening and weakening of the AMOC. The Atlantic basin appears to export water vapor on a ~ 1000 year time scale, which can make the North Atlantic salty enough to be ice-free, with strong heat flux to the atmosphere, sinking in the North Atlantic, and a strong AMOC. If it rains too much or there is excessive river runoff, including from melting glaciers, then the North

Atlantic can get too fresh and will freeze. This shuts off the heat flux, the atmosphere gets cold, and the AMOC slows down. This means that a warm (salty) time of glacial melt implies that in ~1000 years it will be cold (fresh). A cold time exporting vapor implies that in ~ 1000 years it will be warm (salty), with a strong AMOC. This oscillation is a fundamental aspect of the earth system.

This idea is also in accordance with the polar see-saw concept [EPICA 2006; Barker et al. 2009]. The theory argues that cooling to the atmosphere at high latitudes creates a potential for oceanic overturning. If the North Atlantic is slowing then Antarctica takes up the slack. Antarctica and the Arctic oscillated out of phase as the earth system climbed out of the Wisconsin Ice Age. There is a clustering of periods around 1000 years, suggesting a fundamental heat storage time scale. Interestingly, these ventilation events also release old trapped CO_2, which can cause 500 year offsets in radiocarbon dating!

4.3.6. The past 2,000 years

Figure 4.11 shows variations in Greenland surface temperature at GISP2 over the past 2,000 years. Note the relatively warm period during 900 - 1400 A.D. (1100 - 600 ybp), the Medieval Optimum, and the cool period during 1400 -1890 A.D. (620 - 130 ybp), the Little Ice Age. Variations in Antarctica temperature of 2 - 3 K also occurred during the past two millennia (Fig. 4.12) but they appear to be unrelated to variations in Greenland (Fig. 4.11). It seems likely that the millennial variations seen at Greenland are evidence of a climate oscillation that is inherent to the Northern Hemisphere.

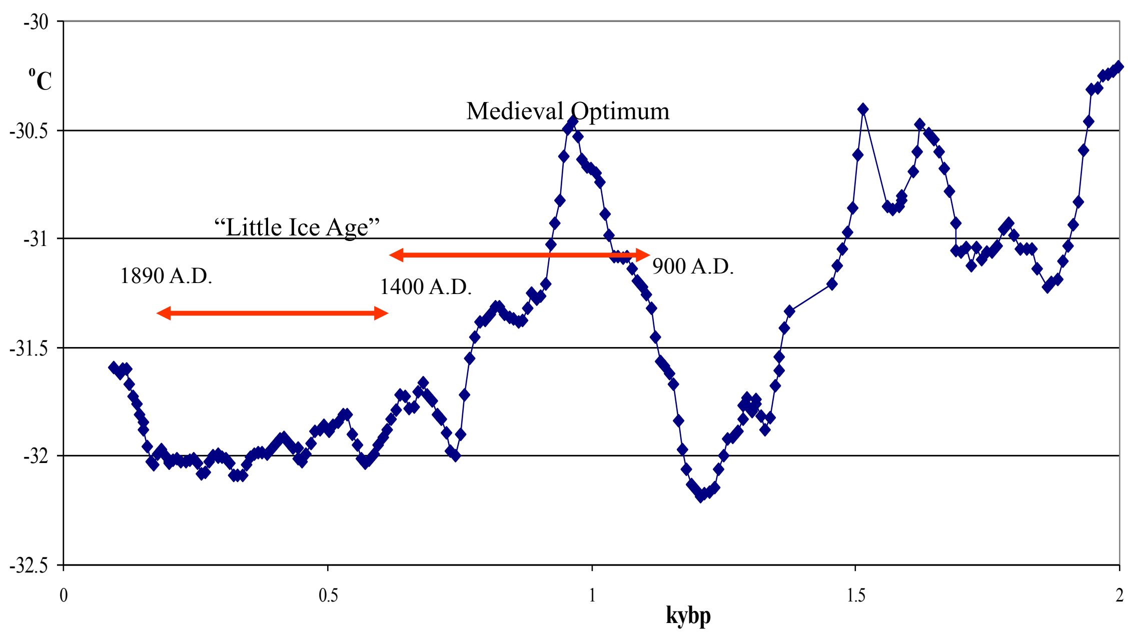

Figure 4.11. Variations in Greenland surface temperature (°C) at GISP2 over the past 2,000 years. Note the relatively warm period during 900 – 1400 A.D. (1100 – 600 ybp) and the cool period during 1400 – 1890 A.D. (600 – 120 ybp) [Alley et al. 2000, 2004, www.ncdc.noaa.gov/paleo].

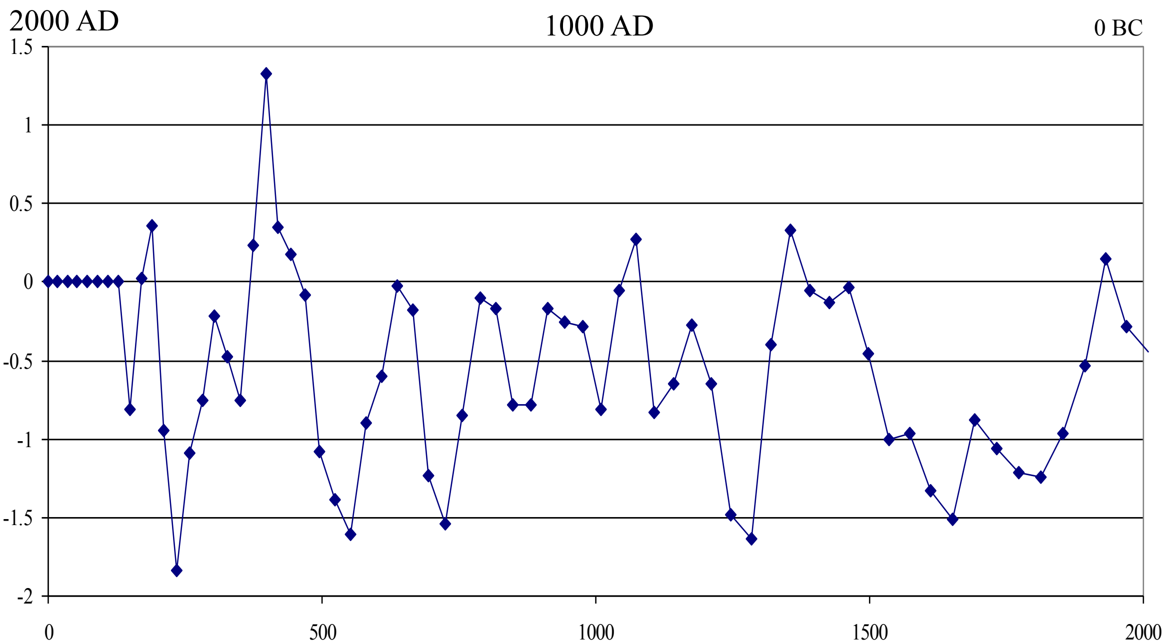

Figure 4.12. Variation of temperature derived from deuterium at Vostok, Antarctica from 2000 ybp to the present (at left) [Petit et al. 2001; data from www.ncdc.noaa.gov/paleo].

During 900-1400 the earth was warm enough for the Vikings to negotiate the North Atlantic more safely and grow food in Greenland. For over 400 years they explored eastern North America and built churches in Greenland with red pine from what is now New England. As the climate deteriorated they may have starved, sailed away, or they may have been victims of the slave trade [Prytz 1991].

During 900-1400 AD, the Southwestern U.S. was warmer than at present. This supported a growing population of Anasazi, which did very well for hundreds of years, but then collapsed after a prolonged dry period near 1130 AD [Diamond 2005]. Periods of drought in this region are influenced by sea surface temperatures in the Pacific and Atlantic and by ENSO [Miao et al. 2007]. A strong ENSO signal began near the start of the Bolling/Allerod warm period (associated with Heinrich event 1), characterized by strong El Nino flooding events in Peru recurring with a 60 to 80-year periodicity. During the Medieval Optimum, a weakened ENSO probably influenced the climate of the Southwestern U.S. [Rein et al. 2005].

Figure 4.13 shows decadal averages of limber pine tree ring width at Italian Canyon, NM (36.4°N, 105.3°W), 2894 m elevation, during 687-1987 AD [Swetnam et al. 1989]. During the period 1090-1170 AD, similar features are seen throughout a broad area of Southwestern U.S. A very profound drought affected the area around 1090, with increasing rainfall around 1100 and 1110, to a noticeable peak around 1120 AD. By this time, the population of the Anasazi had increased considerably, with a complex society centered at Chaco Canyon, NM [Diamond 2005]. The Chaco Canyon Anasazi flourished for five centuries, from 600 A.D. to about 1150 A.D. Their success was fostered by generally warm conditions, but good rains and rapid population growth around 1100 A.D. set the stage for societal collapse, when severe drought set in again in the 1130s and 1140s.

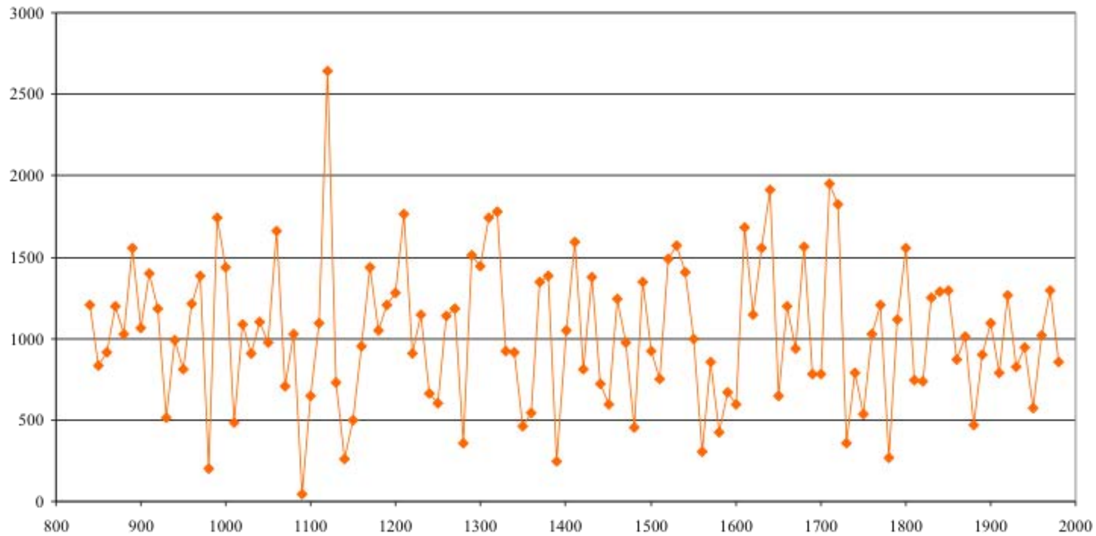

Figure 4.13. Decadal averages of limber pine tree ring width at Italian Canyon, NM (36.4°N, 105.3°W), 2894 m elevation, during 687-1987 AD [Swetnam et al. 1989, www.ncdc.noaa.gov/paleo].

Diamond [2005] elucidates details of the agricultural technology by which the Anasazi succeeded for so long, and ultimately failed. It is interesting to consider whether such ancient events may be lessons for us now. The Anasazi probably understood and discussed their plight, but may not have been able to do much about it, perhaps similar to how we feel today about global warming. Relative to the Anasazi, we benefit from better agricultural technology and a global transportation system that allows us to trade goods over the whole world to compensate for food shortages in some regions. An example of this type of flexibility is the relative imperviousness of United States' food supply in the face of the strong western drought during the past several decades, often exceeding that which occurred in the 1930s.

Is it possible that our global civilization will arrive at a crisis point similar to that which the Anasazi encountered near 1130 AD? During the Little Ice Age, clusters of volcanic eruptions pushed the "advanced western world" to the limits of its ability to feed itself. Two examples of a broad subsistence crisis related to volcanic eruptions during the 1600s and early 1800s will be described below, which remind us that the global population is shaped by climate change. It is encouraging that the population of the world has never declined by more than 15% in its inexorable rise over the past three millennia (Fig. 1.7). This fact lends some security to our collective position and validates the ever-increasing effectiveness of our agricultural technologies. There is cause for concern from at least two quadrants, however. Any perturbation that is large enough to the climate system will be a challenge. As we increasingly disturb the chemical, genetic, and physical environment, unexpected challenges will likely become more frequent and complex.

The Little Ice Age lasted from ~1400 to 1890 and was ~0.6 K cooler than the 1900s, with more severe winters in Eurasia and North America. The Thames and Chesapeake rivers froze more often. On occasion, an Eskimo kayak would show up on the shores of Scotland. Black vultures appeared in dreary Dutch snow-scape paintings. Historians characterize "the general crisis" of the mid-17th century as "adversity on a scale unparalleled in modern times", with numerous wars and popular revolts. Parker [2008] concludes that climate was a major factor, citing Voltaire's explanation to his mistress: "The period of usurpations almost from one end of the world to the other were the result of government, religion, and the climate."

Shortly after Galileo documented spots on the sun that changed over the years, a remarkable period of almost no sunspot activity occurred, the Maunder minimum of ~1620-1715. Given that the sun emits ~0.1% less sunlight during solar minimum compared to solar maximum (Fig. 2.8), this would have contributed toward making the 1600s somewhat cooler. Although this is an interesting theory and probably a contributing factor, the Little Ice Age lasted almost 500 years, including 200 years before and after the Maunder minimum.

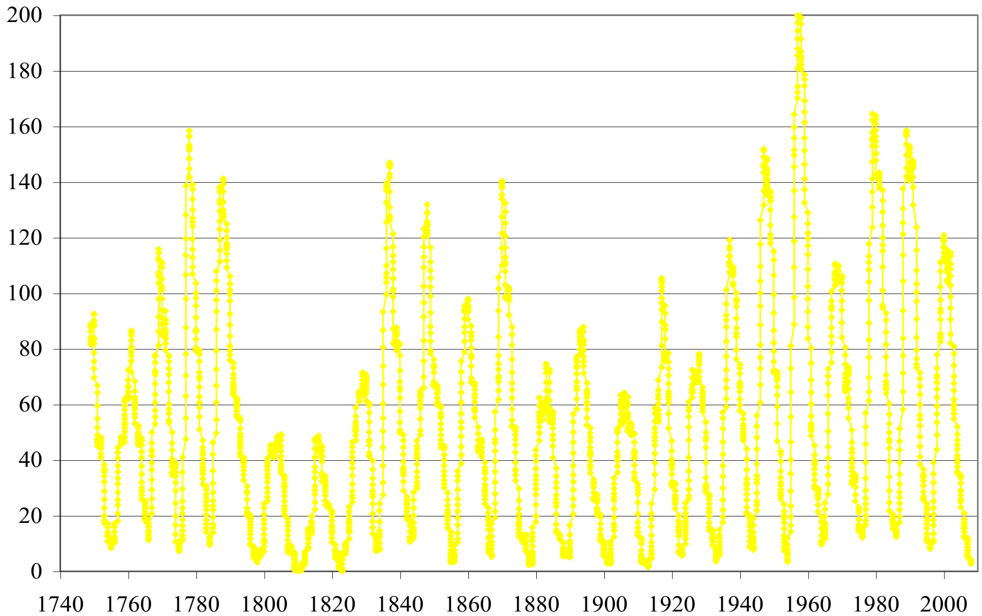

Figure 4.14a. Variation in sunspot number during 1749 – 2009 [from www.ngdc.noaa.gov].

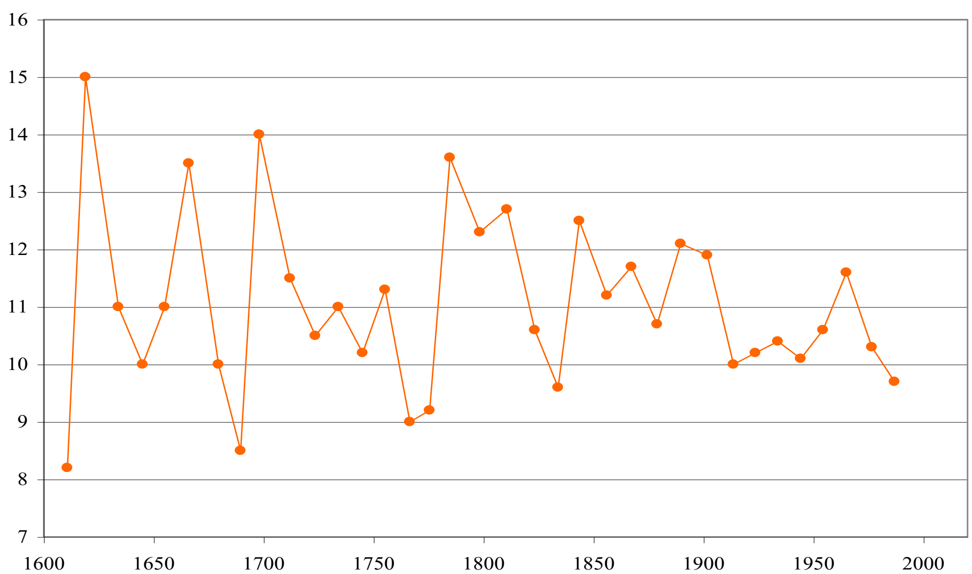

Figure 4.14b. Variation in length of solar cycle during 1600 - 2000 [from www.ngdc.noaa.gov].

The variation in sunspot number and length of sunspot cycle (plotted at the start of each cycle) are shown in Figs. 4.14a, b. The range in solar cycle duration is 8-15 years. The sun may emit slightly more radiation during shorter solar cycles. But the variations in sunspot number and cycle duration in Fig. 4.14b do not seem to have noticeable corresponding features in the temperature signal (Fig. 4.11). The manner and degree to which the solar cycle affects our climate on decadal time scales is poorly understood. However, it is likely that the lack of sunspots during the 1600s contributed to the coolness of that century. What about volcanoes?

Variability of volcanic eruptions can be significant at any time scale, depending on the strength of individual eruptions and the degree of clustering by decade and century [Bryson 1988]. The acidity of Greenland ice cores is a good proxy for global volcanic activity. In the 1-3 years following a major volcanic eruption, particularly tropical eruptions, a thick haze of sulfuric acid droplets form in the stratosphere and reflect sunlight, cooling the planet. These sulfuric acid droplets make their way poleward and downward and become incorporated into snowflakes that fall on Greenland and Antarctica. Counting annual snowfall deposition layers back in time, one can use the amount of sulfuric acid in each snow layer to help diagnose major volcanic eruptions in the past.

The precision of this method is ~1-2 yr, which can be useful for calibrating historical dates. As an example, Fig. 4.15a shows the variation of volcanic sulfate at GISP2 during 1710-1410 BC. Massive eruptions occurred in 1694 BC and 1622 BC, during which time the Minoan civilization thrived. Then came the eruption of Thera (Santorini) in 1453 BC (Fig. 4.15a). Historical forensic methods and radiocarbon dating have greater uncertainty in timing than the sulfuric acid record, but these approaches suggest an end to the Minoan civilization around 1450 BC. Since Thera was located very close to Crete it is likely that its explosion had a serious effect on the Minoan civilization. The date of the acid peak would help calibrate these other methods.

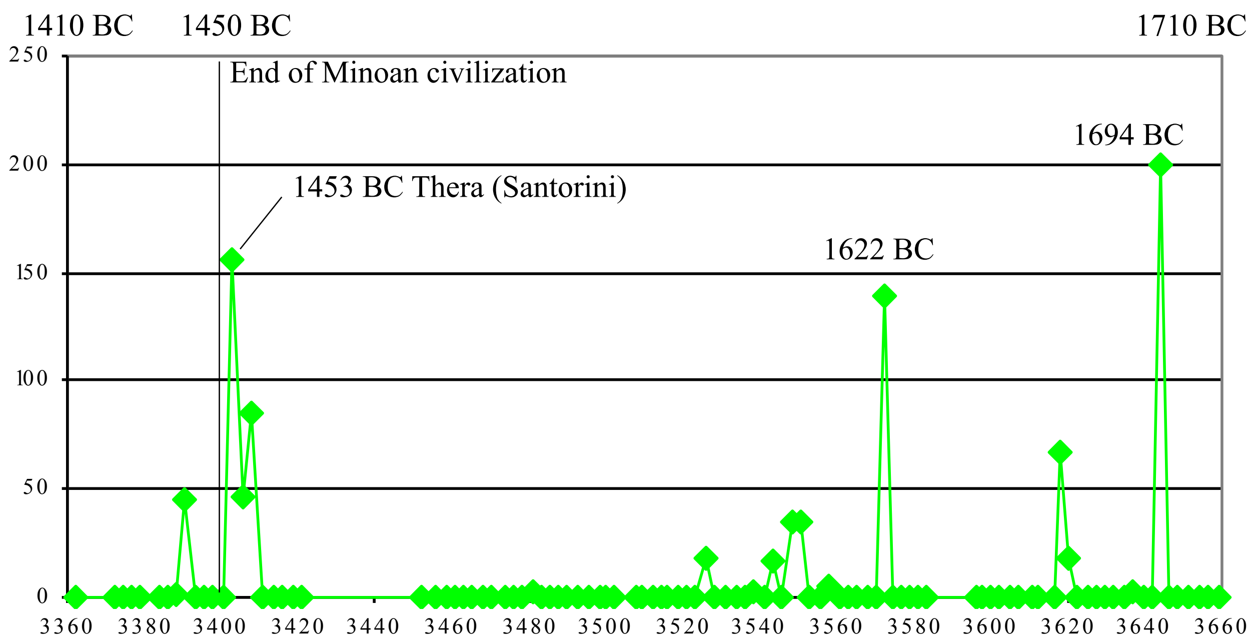

Figure 4.15a. GISP2 volcanic sulfate (ppb) during 3360 3660 years before 1950 AD (1410-1710 BC) [Zielinski et al 1993].

Figure 4.15b highlights the GISP2 sulfuric acid record during 1300 - 1985 AD. A cluster of eruptions started in 1587 and culminated in the massive eruption of Huaynaputina in 1600, which was only to be exceeded by the 1815 eruption of Tambora. Climate proxy data indicate that the earliest part of the 1600s, especially the summer of 1601 was the coldest of the past 600 years throughout most of the Northern Hemisphere [de Silva and Zielinski 1998, Briffa et al. 1998]. The mid-1600s were also a time of repeated volcanic eruptions, notably in 1641, 1660, 1663, 1666, and 1673. More significant climate-altering eruptions occurred during the seventeenth century than in any of the other past five centuries [Briffa et al. 1998]. Although not as pervasive as the 1600s, some historians contend that eruptions in 1783 caused food shortages that contributed toward unrest and the French Revolution [Gore 1993].

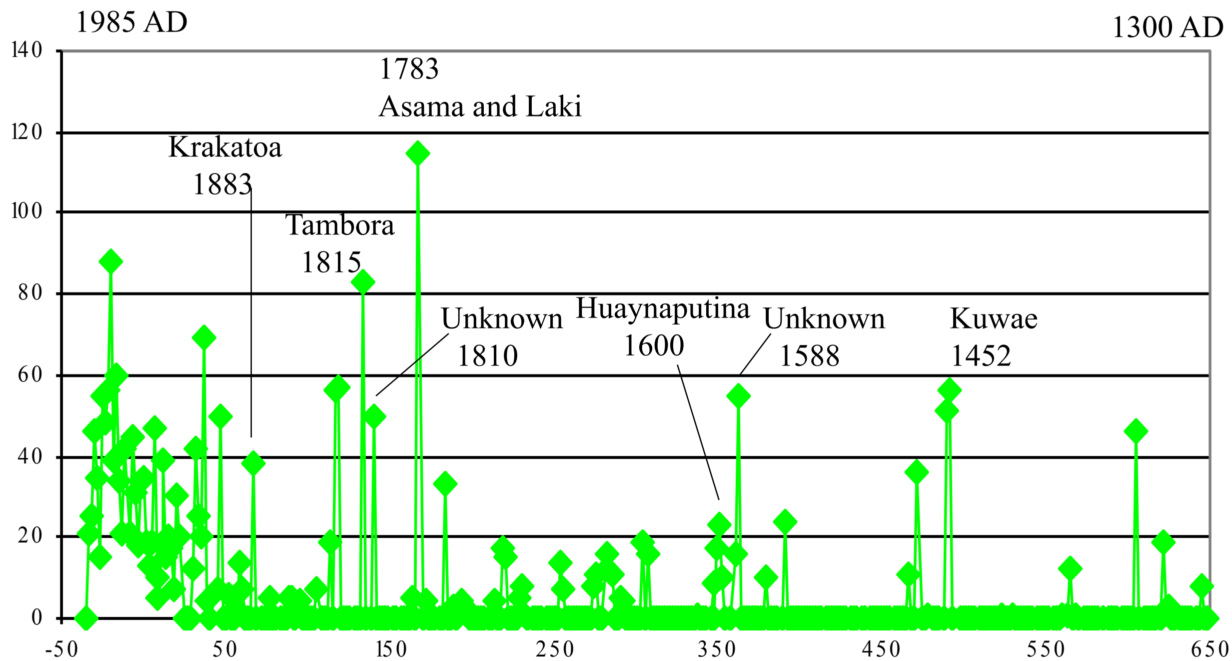

Figure 4.15b. GISP2 volcanic sulfate (ppb) during 650 to -35 years before 1950 AD (1300-1985 AD) from Greenland ice sheet [Zielinski et al 1993].

The eruption of Tambora in 1815 was the largest in the modern era (Fig. 4.15b), one of only four eruptions in the entire Holocene assigned the largest volcanic explosivity index of 7. Over 71,000 people died from it [Oppenheimer 2003]. Instrumental, historical, and tree ring evidence show widespread cold conditions, especially in eastern North America and western Europe in 1816 [Briffa et al. 1998]. The shortest growing season in New England since European settlement was the summer of 1816. Crop failures were widespread, with accelerated emigration from New England and outbreaks of typhus [Oppenheimer 2003].

Strong diminution of Northern Hemisphere tree ring density occurred in the period 1810 - 1820 AD, consistent with another eruption preceding Tambora in 1810 (Fig. 4.15b). The summer of 1816 was the second coldest in the past 600 years, with only the summer of 1601 being colder. The summers of 1817 and 1818 were also quite cold, consistent with the greater time it takes to cleanse the stratosphere of this massive injection of sulfur dioxide into the stratosphere. Briffa et al. [1998] estimate a NH summer anomaly of -0.8 K for 1601 and -0.5 K for 1816.

Large eruptions and closely-spaced multiple eruptions can reduce temperatures on decadal time scales, as occurred in the 1450s, 1600s, 1640s, 1660s, 1670s, 1690s and 1810s. The 1600s were probably unusually cold due to the combination of multiple eruptions and perhaps reduced solar irradiance.

Note the strong increase in sulfuric acid deposition during the 1900s (Fig. 4.15b). This is related to fossil fuel burning and the global dimming which started to reverse around 1980. Climate variations over the last 100 years will be discussed in Chapter 7.

Let us now focus on principles of climate dynamics that can may explain what caused climate variations in the past. We will consider the *Milankovich orbital theory* and *Chaos Theory* in accounting for the glacial / interglacial cycles (section 4.4). The Younger Dryas event is the most recent example of more rapid oscillations that were common during glacial times. The *North Atlantic Oscillator theory* is explored as a possible explanation for these Dansgaard-Oeschger oscillations (section 4.5). Causes of the millennial variability during the Holocene are also explored (section 4.6). Then the effects of volcanic eruptions are revisited, informed by modern observational capabilities (section 4.7).

4.4. Climate Theory and Ice Age / Interglacial Cycles

4.4.1. Milankovich orbital theory

We now consider causes for how our planet wanders back and forth between glacial and interglacial states on time scales of 10,000-100,000 yr. One of the consequences of Kepler's laws is that a planet receives the same amount of sunlight each year (given a constant solar output), regardless of what the axial tilt is or how elliptical the orbit is. Copernicus, Croll, and more recently, Yugoslavian mathematician Milutin Milankovich, studied the manner in which the earth goes around the sun. They felt that by concentrating rays in certain configurations and rarefying them in others, orbital variations can lead to the growth or melting of high latitude continental glaciers. Since most of the land is in the northern hemisphere, the reflective quality of ice will amplify the signal, affecting the average surface temperature of the whole planet.

The equations of motion for bodies orbiting the sun under gravitational attraction have been known since Isaac Newton. Attraction among the planets complicates things, giving minor but significant changes in motion that can accumulate over millennia. Calculation of the motion of objects in the solar system is called celestial mechanics. Over the centuries observations of planetary motion have improved in accuracy, and so has the ability to extend diagnosis of planetary motion into the distant past and into the future. In 1930 Milankovich published an extensive volume which tabulated the intensity of sunlight as a function of latitude and time of year, extending back several hundred thousand years.

The three orbital parameters in the Milankovich theory of climate change are tilt of earth's rotation axis, precession of the axis, and ellipticity of the orbit (Fig. 4.16). When a top is spinning, its axis tilts somewhat off vertical and this pointing direction will gradually rotate around in a circle: its axis will precess. Axial tilt is also known as the obliquity with respect to the plane of the ecliptic. The planets orbit the sun in nearly the same plane, and may eclipse each other in the plane of the ecliptic. A rotation axis that is normal to the plane of the ecliptic would have 0° tilt. Each planet's rotation axis tilts somewhat from the normal, and is oblique with respect to the plane of the ecliptic. Earth's is about 23.5° at present and varies from 22° to 24.5° and back again on a 41,000-year cycle.

The eccentricity of the earth's orbit is about 3.5% at present, implying a 6% variation in solar intensity around the orbit. The eccentricity varies from 3% to 9% and back again on a 100,000 yr cycle. At 9% eccentricity, the solar strength would vary by 20% throughout the year.

The pointing direction of the earth's axis precesses on a cycle of 22,000 yr. At present, the summer sun is in the constellation Aquarius and the axis is pointed toward the star Polaris. Some 11,000 yr from now the axis will be pointed such that the sun will be in the constellation Leo at the summer solstice.

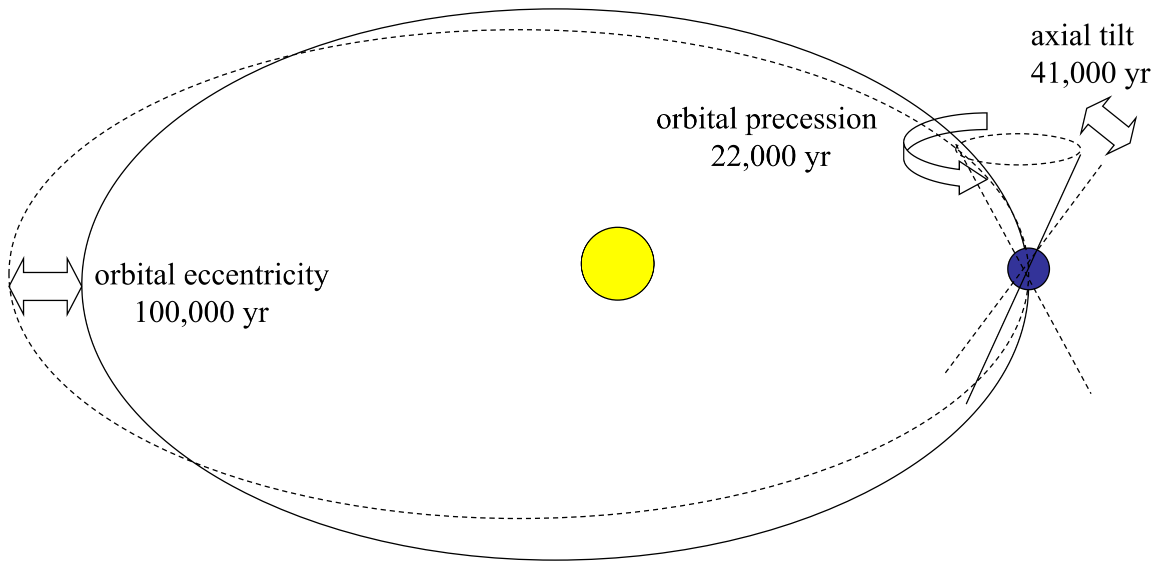

Figure 4.16. Variation in earth orbital parameters as the basis for the Milankovich theory of glacial / interglacial cycles.

If an orbiting planet has non-zero axial tilt then it will have seasons. When a hemisphere is tilted toward the sun, that hemisphere will have summer because the sun's rays are concentrated. When that hemisphere is tilted away from the sun it will have winter because the sun's rays are spread over such a large surface area. This aspect of spherical geometry wins over whether the planet is at a point in its orbit that is farthest or closest to the sun. The precession factor determines where in the orbit northern winter occurs. For example, at present, the least sunlight falls on the northern hemisphere on December 21, which is fairly close to the time of perihelion, or closest approach to the sun, on January 4. Right now, NH winter occurs close to the sun (January 4) and summer occurs far from the sun (July 4). 11,000 years from now NH winter will occur near aphelion, far from the sun.

To understand how the orbital parameters can build up an ice age, we need to consider two aspects of snow accumulation. Firstly, if one assumes that 1 more foot of extra snow is left at the end of each summer, it would take 3000 years to build up an ice sheet 3000 feet thick. This means that there will be a time delay of several thousand years from when optimal orbital parameter configurations begin to generate an ice age and when the ice will be the thickest. The second consideration is that the capacity of air to hold vapor and make more snow depends strongly on temperature (Eqn. 3.1). If air temperatures over a glacier are extremely cold, not much snow can fall. If air temperatures are warmer but still below freezing, more snow can fall. This is the key to understanding how a weak axial tilt favors growth of a glacier.

When axial tilt is weak, seasonal differences are weaker: NH winters are cool and snowy and summers are cool and not much snow is melted. When axial tilt is strong, NH winters are cold and dry, while summers are hot and a lot of snow is melted. Thus, paradoxically, milder seasons favor an ice age!

Figure 4.17 shows the variation of these three orbital parameters during the past 250 ky and the next 100 ky. By considering these parameters alone in a heat balance model for continental glaciers, an ice volume curve such as the lower curve in Fig. 4.17 would be anticipated. The periodicities agree fairly well with the observed climate record (Fig. 4.2). The 100,000 year ellipticity and 41,000-year obliquity periods are compatible with the primary features in the record. More advanced models which include positive feedbacks by greenhouse gases yield a more favorable comparison.

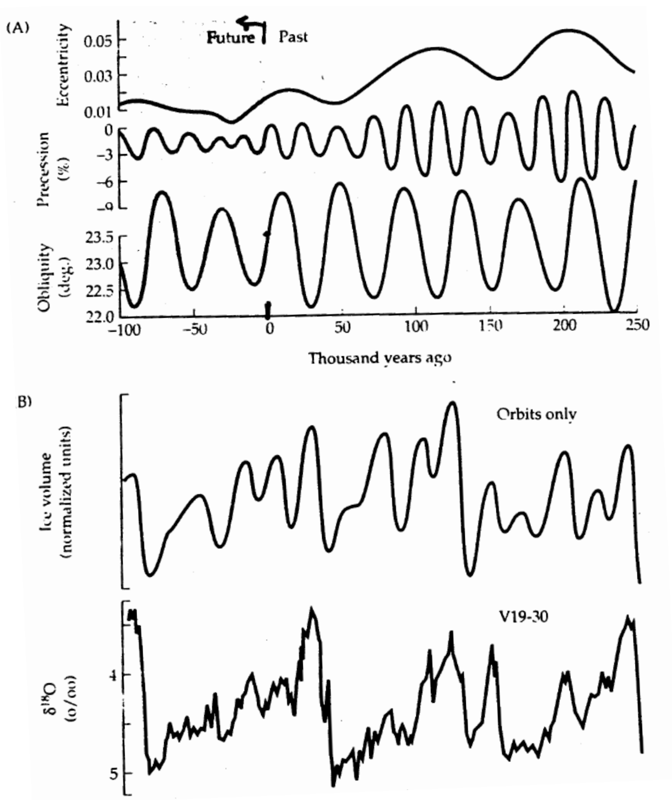

Figure 4.17. a) Past and future changes in orbital eccentricity, precession, and obliquity, and b) estimated effect on ice volume.

The Wisconsin Ice Age began on the heels of a prolonged period of weak axial tilt centered at 25 kybp. We are now entering a similar period of weak axial tilt centered at 5 ky in the future (Fig. 4.17). With the time lag for building up the glacier, a reasonable forecast is an ice age in the 5-10 ky time frame. Milankovich theory supports the Early Anthropogenic Forcing hypothesis, since otherwise we ought to be gradually entering an ice age.

The Milankovich theory of climate change requires amplification of tendencies from orbital parameter variations in order to work. Climate theory allows us to consider idealized states of equilibrium, where there is no net forcing of the climate system to change. A ball-bearing analogue serves to illustrate the types of equilibrium that can exist (Fig. 4.18a). On a flat surface the ball will roll along for a while unchanged. This system is near neutral in stability. At the bottom of a bowl, the shape of the bowl ensures that any perturbation will be opposed and the ball will return to the bottom. This is a stable equilibrium. In the climate system friction, turbulence, and exchange of infrared photons all act to relax the system, to oppose perturbations. Since these factors will act to oppose either a positive or a negative perturbation, they are called negative feedbacks. Negative feedbacks act like stabilizers in the climate system, with a tendency to stay near attractors in climate system phase space.

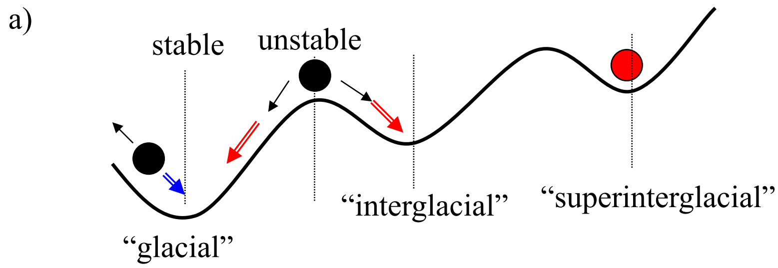

Figure 4.18a. Idealized "ball bearing" model of the stability of the climate system, showing positive (red arrow) and negative (blue arrow) feedbacks to a perturbation (black arrow). Positive feedbacks amplify a perturbation, destabilizing the system away from equilibrium, while negative feedbacks oppose a perturbation, returning the system to normal, thereby stabilizing the system. Three possible climate states are suggested.

On a hill-top a perturbation in any direction will cause a ball to accelerate down the hill. This is an unstable equilibrium. Factors which amplify a perturbation act to destabilize a system. Since these factors act in the same direction as a perturbation, whether it is in the positive or negative sense, they are called positive feedbacks. Positive feedbacks are responsible for wrenching the climate out of its same-old state and pushing it toward a different state.

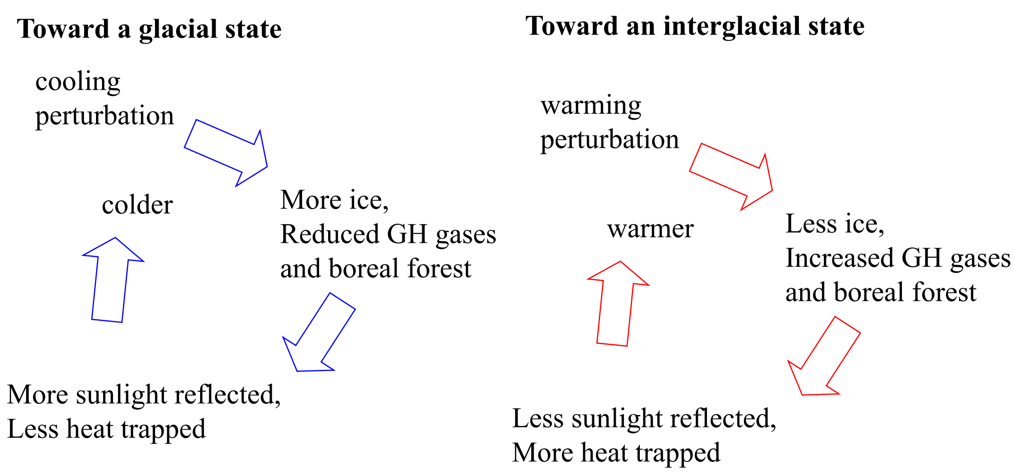

Figure 4.18b. Positive feedbacks in the climate system help cause it to go into an ice age or into an interglacial, acting to amplify a temperature perturbation of either sign. These include the ice albedo feedback, greenhouse gas feedbacks, and the boreal forest feedback.

Positive feedbacks that amplify Milankovich orbital parameters include greenhouse gases, the ice albedo feedback, the boreal forest feedback, and the high latitude soil feedback (Fig. 4.18b). As temperatures increase more water and carbon dioxide evaporate from the oceans, and more methane comes out of the high latitude soils, all creating a stronger greenhouse effect, leading to further temperature increases. As temperatures decrease, water vapor and carbon dioxide condense into the oceans and more methane is frozen into high latitude tundra, weakening the greenhouse effect, leading to further temperature decreases. Meanwhile, a temperature increase will melt snow and ice, allowing more sunlight to be absorbed, warming the periphery further, making things still warmer. A temperature decrease will encourage snow and ice growth, reflecting sunlight, cooling the planet further. Forests trap air and photons, so that if the boreal forest grows farther north, it will trap more heat, further warming high latitudes. If it gets too cold and they die off, their heat retaining properties will be absent, and the planet will get colder.

Positive feedbacks act as amplifiers which help the planet go from one climate state to another. The climate record suggests that glacial and interglacial states represent the extremes of climate, that there may be internal negative feedbacks sufficient to keep the planet within these bounds. To the extent that the complexity of the earth underlies this stabilizing thermoregulatory capability, it seems unwise to continue with massive destruction of ecosystems. By reducing the complexity of the earth organism through species destruction, we may be reducing its resiliency. With the unprecedented loading of fossil fuel CO_2 in the atmosphere, we may be forcing the climate system, like pushing the ball bearing up and over the hill, into a new climate state, a *superinterglacial* state such as has not been seen in the past million years (Fig. 4.18a).

4.4.2. Chaos Theory

But what if these orbital parameters don't actually matter all that much? The climate system is sufficiently complex that one might expect the climate to wander around, with variability at all time scales, including 10,000-100,000 yr time scales. Perhaps the transitions into or out of an ice age are random, with periodicities emerging by chance. This is an argument in favor of internal variability as a source of variation in paleoclimate and future climate, an element of Chaos Theory. Chaos Theory was pioneered by meteorologist Ed Lorenz in 1960. A stimulating synopsis of this rapidly growing field is provided by Gleick [1987].

One aspect of chaos theory is often referred to as the butterfly effect. Lorenz found in his initial numerical weather forecast experiments that, if he changed one input value by an apparently insignificant amount, the new forecast eventually diverged hopelessly from the original forecast. Intuitive aspects of this come from folklore regarding the consequences of a minor change, such as not being able to shoe a horse, being unexpectedly large. The sensitivity of outcome to uncertainty in initial conditions is a central aspect of chaos theory. The ability to forecast the weather will eventually be compromised by whether or not it is known at the outset that a butterfly in Brazil flapped its wings or not. Thus, uncertainty to initial conditions has come to be known as the *Butterfly Effect*.

Jonathan Swift once wrote that

Big dogs have little fleas
That feed on 'em and bite 'em
But the little fleas are plagued by lesser bugs
And so on, ad infinitum
So are the greater poets bit
By the lesser that come behind 'em,

which inspired L. F. Richardson in 1922 to observe that

Bigger whorls have smaller whorls
That feed on their velocity
And small whorls have still lesser whorls
And so on, to viscosity.

This poem represents the idea in chaos theory that the smallest of phenomena are linked to the largest - it's a two-way street. The distribution of large-scale structure helps to determine what happens to individual molecules, while each molecule's behavior determines the whole, not just by additive effect, but by cascade across scale. A butterfly flapping its wings can influence minor zephyrs, which subtly influence larger and still larger zehpyrs, eventually making a slight difference over the whole globe. One may consider the interdependency of civilization and microorganisms in light of chaos theory.

The chaotic nature of even very simple systems is illuminated by Lorenz' simple analog, the water wheel (Fig. 4.19). Imagine a set of leaky buckets mounted in a Ferris wheel configuration, with a water spigot filling them as they pass the top. If the wheel begins to rotate clockwise, more buckets on that side will fill, accelerating the wheel in a clockwise sense. But if it spins fast enough so that the next few buckets don't fill much and the fuller buckets are found on the left side, the wheel may slow down and start rotating the other way. It turns out that it is devilishly hard to predict when the water wheel will reverse its course. It has two states of rotation, clockwise and counterclockwise (two *attractors* in phase space), but one cannot predict when the transition from one to the other will occur; it is chaotic.

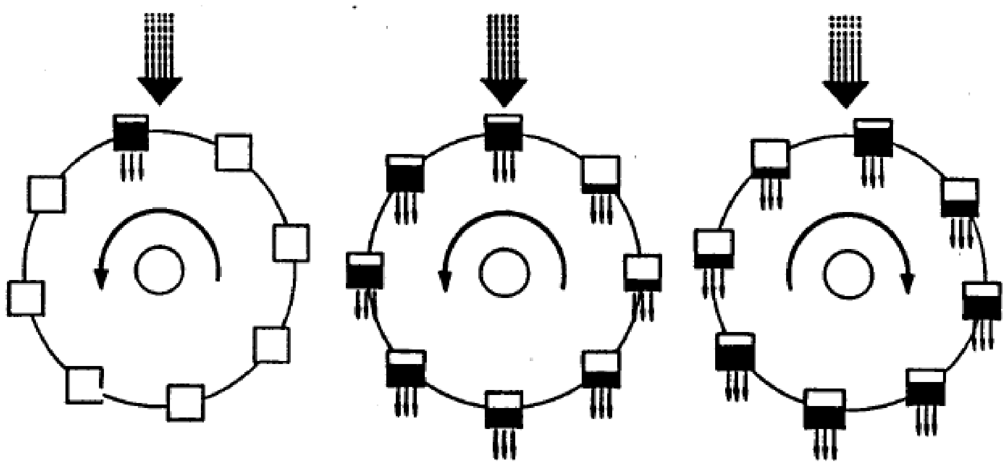

Figure 4.19. The Lorenz water wheel [after Gleick 1987].

Fundamental aspects which contribute toward a lack of predictability, or precise determinism, include Heisenberg's uncertainty principle, phase transitions, advection, hydrodynamic instabilities, and other nonlinear processes. The fact that we cannot determine the precise speed and position of each molecule that makes up the earth system contributes a certain lack of predictability due to the butterfly effect, cascading up from the molecular level. If a raindrop forms and falls, it cannot go back again to where it was. Subtle things may determine whether or not a given raindrop forms. Whether it forms or not represents a great amplification of a small difference. If wind speed varies in space, it will self-advect in a way that changes the distribution. Momentum advection takes the form $u\ \partial u/\partial x$, which is quadratically-dependent on speed, so it is fundamentally nonlinear, a quality that can amplify initial uncertainties. Flow field instabilities include those due to shear and to curvature, which contribute to the chaotic nature of von Karman vortex streets, eddy shedding, energy conversion among eddies, and amplification of waves. Instabilities that seek to lower the center of mass include convective and baroclinic instability associated with growth of synoptic scale storms. Each of these will amplify initial uncertainties, leading to chaotic aspects of weather and climate.

To explore a little further into chaos theory, consider a simple pendulum that is displaced or swung in a circle. Eventually air friction will cause it to come to rest hanging straight down. If you plotted the position of the pendulum in two dimensions on the page it would spiral gradually into the middle. Each perturbation eventually ends up there. The origin is called an attractor in phase space. It is a stable attractor because every perturbation eventually ends up there. Every orbit gradually tends toward that point. It exists due to the negative feedback of friction on the pendulum. In the much more complex climate system negative feedbacks provide regions where the climate spends most of its time. The upper and lower temperatures embodied in glacial and interglacial states represent attractors that arise from friction and infrared emission. The attractors in the climate system are strange, however, because the orbit in phase space is irregular and impossible to predict. They are thus called *strange attractors*.

Lorenz boiled down the climate system into a simple set of three coupled equations governing Rayleigh convection, with three variables being the vertical temperature gradient, horizontal temperature gradient, and amplitude of eddy motion. The famous result from plotting the climate state of this three-variable system in Cartesian coordinates is called the Lorenz butterfly, due to its shape. It features a trajectory around two strange attractors and unpredictable transitions from one to the other. If one substituted equator to pole temperature difference, ice amount, and strength of poleward heat transport, and plotted their variation over geologic time, one would see a pattern emerge which clusters around glacial and interglacial times, with transitions between the two being unpredictable. The AMOC exhibits a cyclic variability at ~1000 year time scale, with hysteresis effects that are partly predictable, but its observed variation is also consistent with chaos theory, where the exact times of transition are unpredictable.

Since elements of determinism and chaos were both present in the initial moments after the Big Bang, it makes sense to describe climate dynamics as having a healthy mixture of both. Milankovich theory goes a long way toward describing the fundamental climate signal over the past million years, but the detailed evolution of the earth's climate has chaotic qualities to it. One aspect of the climate signal that begs explanation is the fact that Dansgaard-Oeschger events have been very weak during the past 10,000 years. Even during the Emian interglacial there were chronic rapid oscillations, near the bottom of the ice core in Fig. 4.2. What is the secret to the stability of the late Holocene?

4.5. Strong climate oscillations during the Ice Ages

Strong oscillations in Northern Hemisphere temperatures are a hallmark of the ice ages [Dansgaard 1982]. The rapid warming phase is accompanied by Heinrich events of rafted rock debris. The last of these Dansgaard-Oeschger events included the Bolling/Allerod warm period, the Younger Dryas cool period, and the rapid warming around 11.6 kybp.

Broecker [1992] hypothesized that these events are caused by fresh water flooding of the North Atlantic leading to changes in the thermohaline circulation, which has a natural time scale of many hundreds of years, the North Atlantic Oscillator hypothesis. One possible sequence starts with the retreat of the Laurentide ice sheet, which allowed water from Lake Agassiz in south central Canada to flow out the St. Lawrence river. This influx of fresh, light water may have been sufficient to stop the formation of North Atlantic bottom water and direct the Gulf stream away from Scandinavia toward Spain. This could have led to cooling of the North Atlantic and subsequent regrowth of the Laurentide Ice sheet. The timing of release of stored greenhouse gases from various ecosystems may have contributed to these oscillations.

The idea that changes in the Gulf stream and bottom water formation can exert a strong control over climate underpins the movie Day After Tomorrow, in which anthropogenic global warming induces an ice age all of a sudden. The primary difference between the current situation and that of 12,000 years ago is that the Laurentide ice sheet was still large and ready to grow but today it is gone. Moreover, the strength of the Gulf stream is controlled primarily by by the pattern of wind stress over the Atlantic basin, so it is not clear that the Gulf stream would weaken significantly if the formation of deep water ceased. Nevertheless, if the Gulf stream penetrates farther north, as it does now, it is consistent with a warm arctic. When the Gulf stream landfalls in southern Europe it is consistent with a cold arctic. Because of the proximity of the Canadian shield, which can build up snow, the North Atlantic is the seat of powerful climate change. The interaction among the atmosphere, ocean, and cryosphere is subtle and not well understood, yet therein lies the key to the Dansgaard-Oeschger events which dominate the climate record during glacial times.

4.6. Millennial variations during the Holocene

As a primary driver behind Milankovich theory, Northern Hemisphere summer insolation at 60°N in June was ~40 W/m^2 stronger 11 kybp compared to the present, when Northern Hemisphere summer occurred at perihelion. These hot summers mass-wasted the continental glaciers and it got warmer. Drainage from Lake Agassiz at the edge of the retreating Laurentide Ice Sheet in southern Canada flowed through the Great Lakes and out the St. Lawrence river. During 11.7-8 kybp the environment of the Great Lakes was cool and dry, with lake levels considerably below basin outlets [Lewis et al. 2008]. Overflow surges occurred about a millennium apart during the warm and wet times.

Similar millennial variations are seen in the strength of the Asian monsoon and the North Atlantic throughout the Holocene [Gupta et al., 2003]. Cool episodes in the North Atlantic are accompanied by weakening of the Asian southwesterly monsoon wind, while a warm North Atlantic coincides with a strong Asian monsoon. Since this relationship also held for the larger Dansgaard-Oeschger cycles during the last glacial period, it would seem to be a natural mode of variation of the climate system. The Medieval Optimum and Little Ice Age are but the most recent manifestation of this fundamental variability of the earth system. Hence, sunspots and volcanoes have important effects, but the millennial variations seem to be more fundamental.

The quasi-millenial periodicity may be related to natural time scales in the earth system, such as thermohaline overturning and ocean heat storage, the growth and decay of ice sheets and vegetation, and rates of release or sequestering of greenhouse gases. Yet the determinist in us yearns for a more satisfyingly direct causal explanation. Variations in cosmic rays at this time scale must be used to correct radiocarbon dates. Based on this and other evidence, some scientists have speculated that there is some object, perhaps a terrible comet in a very long orbit which induces climate change at millennial periodicities.

In a discussion of the Holocene and cyclical events it would be remiss to ignore the cultural fascination that is occurred with regard to December 21, 2012. The Mayan calendar is the most exact calendar ever devised, and has been in existence since at least 600 BC. The Mayan Long Count is based upon the number of elapsed days since a mythological starting-point. According to the correlation between the Long Count and Western calendars accepted by the great majority of Maya researchers, this starting-point is equivalent to August 11, 3114 BC. The Long Count is based on detailed observations of the sun, moon, and Venus. One cycle in the Long Count repeats every 144,000 days, or about 400 years, which is 1 Baktun. The Mayans also probably monitored the behavior of Jupiter and Mars. A longer cycle repeats every 5125 yr, with the ending point on December 21, 2012. Nostradamus predicted the appearance of a terrible comet after the year 1999, with subsequent societal chaos. This seems to have fueled a wide and diverse array of speculations about the 2012 Problem, with the end of a Mayan cycle being invoked as a lynchpin in the argument. However, the beginning of the Mayan calendar predated its invention by 2500 years, and the 5125-year cycle length depends in part on the Mayan preference for base 20. Just to spice up the mixture, in the attempt to understand the fundamental nature of the universe through high-energy particle collisions, physicists assure us that we will find probably find a Higgs boson through the formation of a “small black hole” at the collider in France by 2012. “May you live in interesting times!”

4.7. Volcanoes and Climate

Volcanic eruptions can cool the planet for several years, lead to more PSCs and cirrus, exacerbate ozone depletion, and can change weather patterns. Figure 4.20 summarizes the primary effects of small tropospheric eruptions and of large volcanic eruptions that reach the stratosphere. Eruptions can consist of an array of ash particles, with smaller particles carried farther by the wind. On geological time scales, wind-borne volcanic ash is a significant source of mineral nutrients for islands far out at sea. The primary gaseous emissions are H_2O (85%), CO_2 (15%), and trace amounts of N_2, HCl, H_2S, and SO_2. The sulfur gases from minor tropospheric eruptions become oxidized into sulfuric acid, incorporated into liquid sulfate aerosol and precipitate out within 1-3 weeks. This is similar to the fate of fossil fuel sulfur and acid rain.

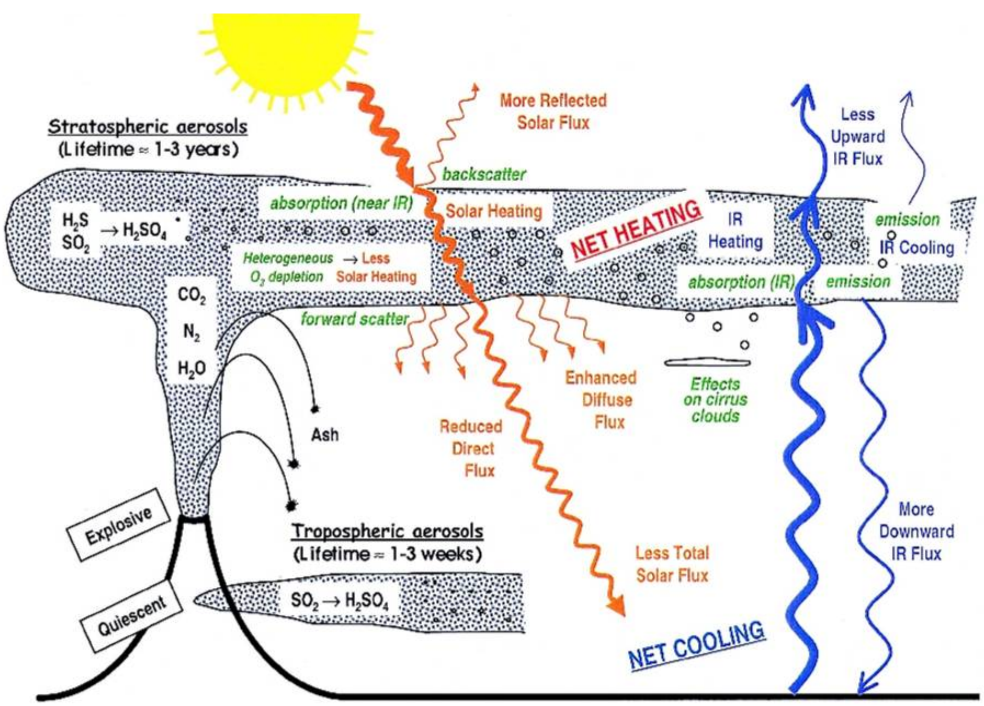

Figure 4.20. Volcanic effects on the atmosphere [from Robock 2000].

A large eruption can inject gases directly into the stratosphere, where it takes about 6 months for sulfur compounds to form the characteristic volcanic stratospheric sulfate aerosol, with bright orange sunsets. This stratospheric aerosol layer is known as the Junge layer, with a maximum mixing ratio near 21 km in the tropics (Fig. 4.21). Volcanically-enhanced sulfate aerosol can remain for 1-3 years or longer, with an exponential decay rate of ~1/e in 22 months. The dominant effect of stratospheric volcanic aerosol is backscattering of solar visible and UV to space, cooling the surface of the planet. The aerosol layer acts as a greenhouse agent, absorbing upwelling surface infrared, heating the bottom half of the aerosol layer. This can lead to lofting in the tropics and an enhancement of the overturning Brewer-Dobson circulation. Volcanic eruptions provide unique insights into the general circulation of the stratosphere and troposphere. They are also harbingers of changing weather, notably warmer winters in the interiors of the continents of North America and Eurasia.

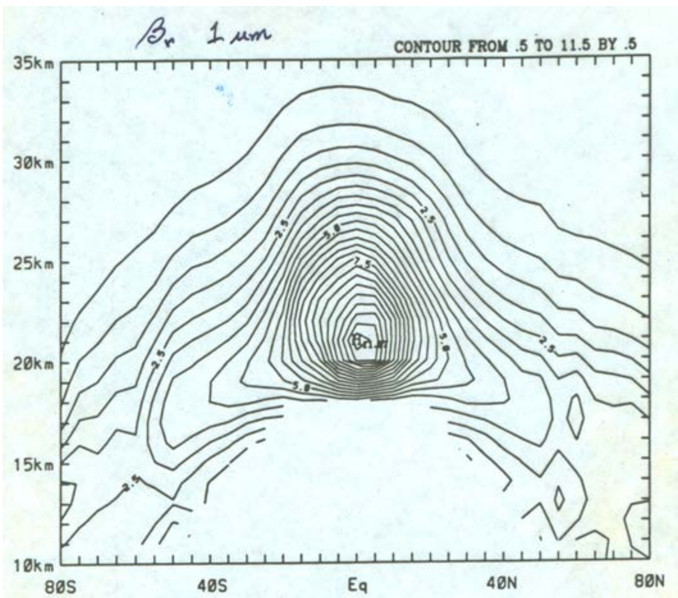

Figure 4.21. Decadal mean volcanic aerosol extinction ratio [Hitchman et al. 1994].

Sometimes a distinctive volcano can be a vital geographical marker. According to Herodotus, in 600 B.C. Pharoah Necho II sent ships clockwise around Africa and back through the Straits of Gibraltar to the Nile [Hermann, 1932]. On a similar circumnavigation in 500 B.C. Captain Hanno commented specifically on the location of Mt. Cameroon near the equator on the west side of Africa. Francis Drake mentioned that Mt. Cameroon was erupting when he passed by to harass Spanish vessels on the west coasts of the Americas in 1587, then exploring the Pacific Northwest for the fabled Northwest Passage. If only he had been born today he could have realized his dream of sailing the Northwest Passage.

Pesky Icelandic volcanoes have been the bane of agriculture and cause of famine many times. In 1150 B.C. Hecla 3 erupted and the population of Scotland dropped 90% due to failed crops (Gore 1992). Chinese scholars noted at the time that “it rained dust at Po”. Again in 208 B.C., an Icelandic volcano caused the scholars to write “stars were not seen for 3 months” and there was a great famine in China the next year.

Around 1783 there were multiple eruptions of Mt. Asama in Japan and furious fumigations from Loki in Iceland. Icelandic eruptions do not generally reach the stratosphere by direct injection. Yet material can be transported into the lower stratosphere near weather systems. Moreover, it has been realized recently that particles can absorb infrared, making the air warmer and lighter, and loft, making its way into the stratosphere. Forest fire smoke in

Canada has been observed to self-loft into the summer stratosphere. It is likely that some of the Loki material made its way into the stratosphere. This was followed by 6 years of crop failures in Europe. It may have fostered unrest and contributed toward conditions leading to the French Revolution.

Mt. Tambora erupted in 1815. The next year has gone down in history as "the year without a summer". It snowed in New England in July. There was a famine in Europe in 1817 and 1818. The result has been called "the last great subsistence crisis in the Western World".

Then on August 27, 1883 Krakatoa erupted, sending enormous tsunamis that killed 35,000 people. For several hundred years, passersby would refer to Krakatoa as "an island with a pointy mountain" [Winchester 2002]. In 1858 Alfred Russell Wallace was in the vicinity, documenting an astounding 125,660 new species in Indonesia. He had great insights into the idea of survival of the fittest, a driving force in evolution, and sent a formal manuscript on the subject to his mentor Charles Darwin to deliver to the Royal Society. Darwin was far into writing his book *On the Origin of the Species* and felt quite discomfitted. In the end, he presented both works to the society. Wallace didn't seem to mind the early lack of recognition of this contribution, preferring to continue collecting new species. He also had astounding early insight into the idea of continental drift. He knew that there must be some way to explain the abrupt juxtaposition of Eurasian species and Australian species across a deep north-south channel near Bali. This line has come to be known as the Wallace Line. It wasn't until the end of the century that famed meteorologist and geologist Alfred Wegner posed his theory of continental drift. Now we know that the oceanic plates diving under Indonesia make for an unusually explosive brand of volcanic eruption.

On August 27, 1883 Captain Thompson of the British ship Medea measured the height of the volcanic cloud to be no less than 17 miles or 27 km, well into the stratosphere. As the sun never set on the British empire, Royal society observers reported brilliant orange sunsets in a pattern spreading westward from Indonesia in the tropics. Scientists concluded that stratospheric winds were westward, and referred to them as the "Krakatoa easterlies". After a few months, northern winter began setting in, and the eruption cloud began to transported northward into the winter westerlies, with orange sunsets arriving from the west over Britain some 3 months later. This informs us that volcanic aerosol tends to be confined to the tropics, and will spread poleward by wavy variations in the stratospheric jet stream during winter.

People were content with the volcanically-informed notion of "Krakatoa easterlies" for several years. Then in August of 1908 Arthur Berson made careful measurements of winds and temperatures at Dar es Salaam at 6.3°S and Shirati at 1°S, using radiosonde balloons that could reach the tropical lower stratosphere. That is hard to do, since the tropopause is quite high over tropical Africa. On August 30 at Shirati the coldest temperature was -84.3°C (188.7 K) at 19,330 m. Much to everyone's surprise, Berson found weak westerly winds in the layer 19-20 km. The new view became a layer-cake, with steady deep Krakatoa easterlies topping a thin layer of Berson westerlies.

It wasn't until Reed et al. (1961) discovered a most interesting phenomenon that all was revealed. By systematically examining long time series of radiosonde observations in tropical stations they were able to deduce that westerly and easterly wind regimes formed and descended in time, to be repeated again in a cycle taking 24-32 months (Fig. 3.32). The QBO is not driven by the annual solar cycle. Instead it is driven by the upward transport of momentum by tropical waves above deep convection. The QBO exerts a strong influence on stratospheric circulation and has an influence on tropospheric weather as well. It turns out that a volcanic eruption serves as a perfect dye for illuminating the circulations associated with the QBO.

There are various ways of estimating the magnitude of influence of volcanic eruptions, including a severity index, a volcanic explosivity index, and aerosol optical depth observed at the surface. Table 4.1 shows the major eruptions of the past 150 years. Figure 4.22 shows an estimate of aerosol optical depth during that time, based on severity and explosivity indices [Sato et al. 1993]. Ground-based pyrheliometers provide a more direct means of estimating volcanic eruptions (Fig. 1.8). Note the huge eruption of Krakatoa (1883) and the clustering of eruptions in 1880-1915 in both data sets, a period when the earth was fairly cold. The 1930s and 40s were fairly devoid of eruptions and these were warm decades. In the pyrheliometer data of Goodman [1980] a gradual rise in aerosol optical depth occurred from 1940-1970. This is referred to as the global dimming, and may be related to the sulfate aerosol produced by burning fossil fuel (see section 6.3).

Date	Volcano	Latitude, Longitude	Severity	VEI
1854, Feb.	Sheveluch, Kamchatka	57°N, 162°E	...	5
1855–1856	Cotopaxi, Ecuador	1°S, 78°W	1.5	...
1856, Feb.	Awu, Celebes	4°N, 125°E	2	...
1861, Dec.	Makjan, Molucca Islands	0°N, 127°E	2	4
1875, March	Askja, Iceland	65°N, 17°W	2	5
1883, Aug.	Krakatau, Indonesia	6°S, 105°E	1	6
1886, June	Tarawera, New Zealand	38°S, 177°E	2	5
1888, March	Ritter Island, Bismarck Archipelago	6°S, 148°E	2	...
1888, July	Bandai San, Japan	38°N, 140°E	2	4
1892, June	Awu, Celebes	4°N, 125°E	2	...
1902, May	Mont Pelée, Martinique	15°N, 61°W	2	4
1902, May	Soufrière, St. Vincent	13°N, 61°W	2	4
1902–1904	Santa Maria, Guatemala	15°N, 92°W	1.33	5–6
1907, March	Shtyubelya, Kamchatka	52°N, 158°E	2	5
1912, June	Katmai, Alaska	58°N, 155°W	2	6
1932, April	Quizapu, Cerro Azul	36°S, 71°W	3	5
1947, March	Hekla, Iceland	64°N, 20°W	2	4
1953, July	Mount Spurr, Alaska	61°N, 152°W	2	4
1956, March	Bezymyannaya, Kamchatka	56°N, 161°E	2	5
1963, March	Gunung Agung, Bali	8°S, 116°E	1.5	4
1966, Aug.	Awu, Celebes	4°N, 125°E	2	4
1968, June	Fernandina Island, Galapagos	0°S, 92°W	2	4
1980, May	St. Helens, United States	46°N, 122°W	...	5
1982, April	El Chichon, Mexico	17°N, 93°W	...	5
1991, June	Pinatubo, Philippines	15°N, 120°E	...	5
1991, Aug.	Hudson, Chile	46°S, 73°W	...	5

The severity numbers 1, 2, 3 of *Mitchell* [1970] are intended by the author to represent volumes of ejecta 1–10, 0.1–1, 0.01–0.1 km^3, respectively. Volcanic explosivity index (VEI) numbers 6, 5, 4 of *Newhall and Self* [1982] are intended by the authors to represent volumes of ejecta 10–100, 1–10, 0.1–1 km^3, respectively.

Table 4.1. Volcanoes in the period 1850-1991 of severity class 2 or higher [Sato et al., 1993].

The eruption of Mt. Agung in 1963 ushered in another few decades of moderate volcanic activity, including Mt. St. Helens in 1980, El Chichon in 1982, and Mts. Pinatubo and Hudson in 1991. These years were not particularly hot years. Since Mt. Pinatubo there has not been a major eruption and it has gotten warmer. It seems likely that some of the record high temperatures in the last decade can be attributed to the lack of volcanic eruptions.

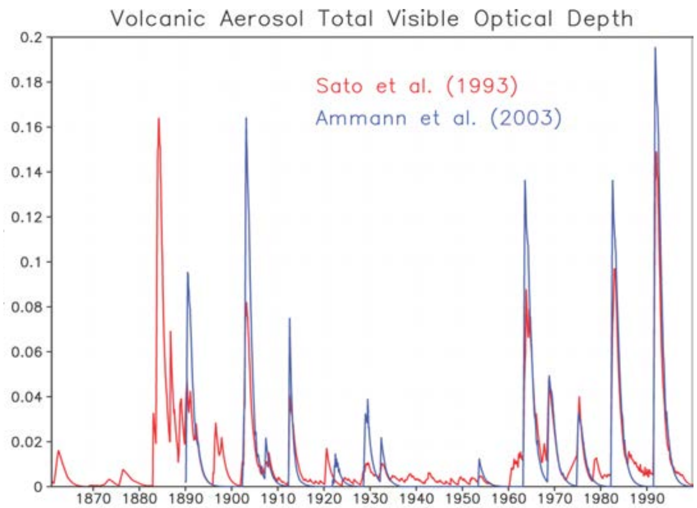

Figure 4.22. Aerosol optical depth over the past 150 years [IPCC 2007].

Focus: the eruption of Mt. St. Helens

While living in Seattle in 1980 I used to go sailing on Lake Washington and watch Mt. St. Helens send up big clouds of material. A fellow graduate student named Keith Ronnholm used to go down to a ridge north of Mt. St. Helens each weekend between classes and take pictures. Inclinometers showed that the north face was bulging outward and that something interesting might happen. He felt fairly safe 20 miles away. At 9 o'clock on the morning of May 19 people started screaming, so he scrambled out of his tent and took a few pictures (Fig. 4.23a). Then he dove in his pickup truck and headed north down the logging roads away from the debris cloud, which was advancing at 150 mph. Luckily, he got behind a ridge, but it kept getting closer and closer (Fig. 4.23b), until he was enveloped in falling ash and it became completely dark. The ash kept building up, 6″, 8″, 10″, until he thought he would suffocate. Then a knock on his car door in the dark revealed a logging truck with three men, one to drive, and one each to feel for the ditch with his feet in the dark. Keith got in right behind them and could see their bumper when about 1′ away and followed them out to the town of Randle. He was not one of the 35 killed by Mt. St. Helens that day.

Figure 4.23. Eruption of Mt. St. Helens, May 1980 [photos by Keith Ronnholm].

A latitude-time section of stratospheric aerosol (Fig. 4.24) shows the eruptions of Mt. St. Helens, Ruiz, El Chichon, Hudson, and Pinatubo. Extratropical eruptions tend to be cleansed fairly rapidly by the Brewer-Dobson circulation transporting the aerosol poleward and downward, where it is lost in the troposphere. This is why Mt. St. Helens didn't have much of a cooling effect planet-wide. As the plume made its way across the U.S., wherever the cloud was thickest, the daytime maximum temperature was reduced by a few degrees, due to solar reflection, and the nightime minimum was also reduced, due to infrared trapping.

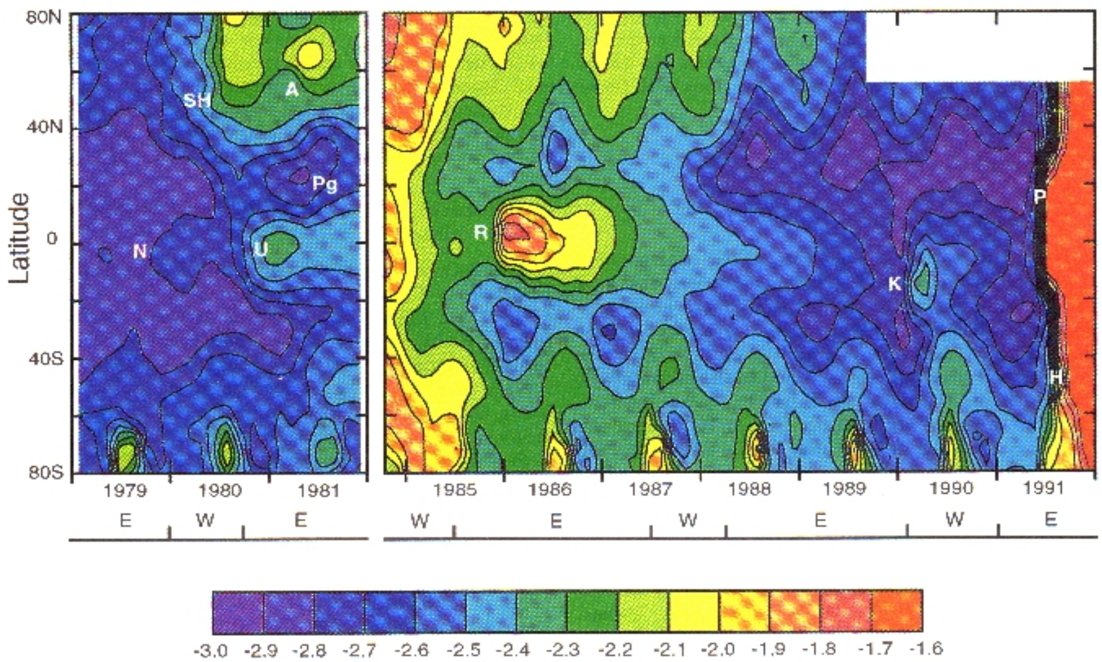

Figure 4.24. Latitude time section of stratospheric aerosol optical depth at 1 μm. The logarithm of optical depth is shown in color. Letters indicate specific volcanic eruptions. The phase of the QBO is also shown [Hitchman et al. 1994].

One may also see that aerosol tends to come out of the tropics during winter and during the westerly phase of the QBO. Figure 4.21 shows the mean distribution of aerosol. It peaks near 21 km altitude in the tropics. Within a year after an eruption the pattern looks very similar to this. Note the poleward and downward extension from the tropical aerosol reservoir in the lowest stratosphere.

Figure 4.25 shows how the Pinatubo cloud spread westward in QBO easterlies, making a ribbon shape in the tropics. It was confined to the tropics until winter set in. Figure 4.26 shows that the arrival of volcanic aerosol in the lower stratosphere over Colorado in the midlatitude westerlies didn't occur until October of 1991, but the eruption was in June. This is similar to the sequence observed after Krakatoa.

The effects of volcanic eruptions on PSCs (see section 5.3) is very noticeable in Fig. 1.9, which shows the evolution of optical depth in the Arctic and Antarctic. After the eruption of El Chichon there was much more aerosol mass in the Arctic, and the PSCs in the southern winter began much earlier in the year.

Eruptions heat the tropical stratosphere by 1-4 K, causing an acceleration of the Brewer-Dobson circulation. By cooling the troposphere, the tropical tropopause will not be forced by convection to be so high and cold, allowing more water vapor to enter the stratosphere, further changing the radiative budget.

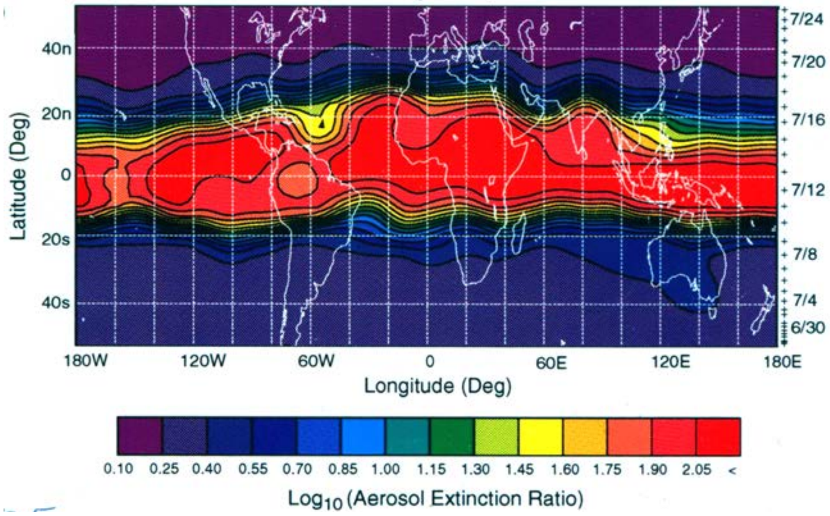

Figure 4.25. Volcanic aerosol pattern in early July 1991 near 21 km altitude after the eruption of Mt. Pinatubo in May 1991 [Trepte et al. 1993].

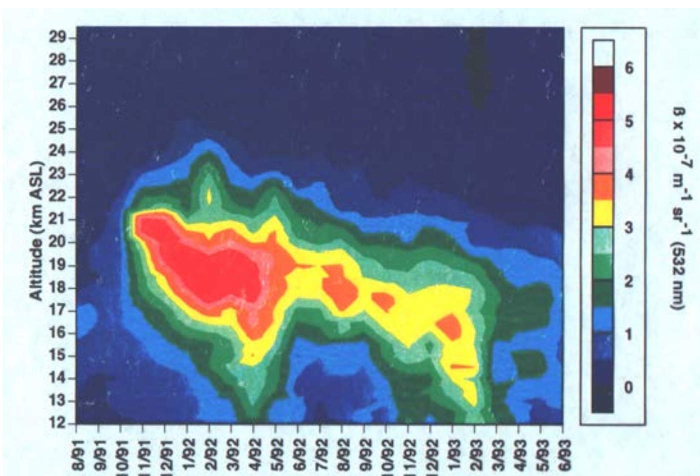

Figure 4.26. Time-altitude section of monthly mean lidar backscatter at 0.532 μm at Fritz Peak Observatory, CO, after the eruption of Mt. Pinatubo [Langford et al., 1994].

There is an interesting consequence stemming from the fact that the tropical stratosphere warms more than high latitudes, resulting in a stronger westerly jet in the midlatitudes. In winters following a major eruption, instead of the jet stream setting up in a continentally-fixed standing wave pattern, the subtropical westerly jet is stronger and comes from the Pacific ocean more directly into the Midwest, while the Atlantic jet stream goes right across Europe into Russia. The result is to bring warm air from over the North Pacific and Atlantic into the interiors of continents, keeping them warm. Thus, while the globe cools generally after an eruption, during the winter the interiors of continents are warmer [Robock, 2000].

A volcanic eruption can also excite the NAM and the SAM (section 3.9), since a stronger westerly vortex favors the high index phase of each. We now know that a strong vortex regime in the northern winter stratosphere is a good predictor of a strong westerly vortex in the troposphere over the next several weeks [Thompson and Wallace, Baldwin and Dunkerton 2000]. This may be the mechanism by which warm continental winters are obtained.

Key Terms

AMOC – Atlantic meridional overturning circulation, varies at 1000 yr time scales
attractor – preferred region in phase space for a system
chaos theory – imperfect information and complexity lead to unpredictability
climate dynamics – study of the processes by which climate change and climate stability occur
Bolling - Allerod – warm period 14.6 – 12.9 kypb (thousand years before present)
boreal forest feedback – a positive feedback
butterfly effect – imperfect knowledge of the initial state implies unpredictability
Cretaceous – warm period during 150 – 65 Mybp, when sea level was much higher
Dansgaard - Oeschger events – large-amplitude quasi-millennial periodicity during an Ice Age
dendrochronology – using patterns of annual tree-ring growth as a climate clock
determinism – theory that the laws of physics precisely determine the outcome
early anthropogenic hypothesis – we changed the albedo of the planet to prolong the interglacial
Emian Interglacial – the last previous interglacial warm period, during 130-115 kybp
end of millennium warming – rise in global temperature by ~1 K since ~1900 A.D.
faint young sun paradox – 75% weaker sun 4 Bybp but no "ice-ball earth"
Gaia hypothesis – life on earth collectively stabilizes the climate system
geoengineering – human manipulation of the earth system to alter the climate
greenhouse gas feedback – positive feedback by gases which amplify a perturbation
Heinrich events – short periods of massive ice-rafted rock debris in the North Atlantic
high latitude soil feedback – possibly positive feedback of methane release and sequestration
Holocene – warm interglacial period since the Younger Dryas, 11.6 kypb - present
hosing event (meltwater pulse) – rapid melting of continental glaciers
North Atlantic oscillator theory – deep water formation is anti-phased between hemispheres
isostatic rebound – when continental ice sheets melt land beneath rises by Archimedes' principle
Laurentide Ice Sheet – North American ice sheet reaching maximum near 20 kybp
lichenometry – using the size of lichens to determine age of exposure of a rock surface
Little Ice Age – cold period during 1400-1890 A.D.
Medieval optimum – warm period during 900-1400 A.D.
Milankovich theory – ice ages controlled by periodicities in ellipticity, axial tilt, and precession
Oort cloud – hypothesized region where comets loosely orbit the sun outside of the solar system
radiocarbon dating – use of 5400-yr half-life of ^{14}C to determine age of organic material
strange attractor – preferred region in phase space where the same sequence is never repeated
Younger Dryas event – cold period during 12.9-11.6 kypb
varve – annual layer of sediment in lakes containing pollen and other information
Wisconsin Ice Age – cold period during 100 – 17 kypb

Thought Problem

Paleoclimatologists agree that there is a see-saw between oceanic convection in the North Atlantic and in the circumpolar Antarctic on a time scale of about 1000 years. As the global average temperature rose from the last ice age maximum about 20,000 years ago to the beginning of the Holocene about 8,000 years ago, surface temperatures over Greenland and Antarctica oscillated up and down with ~1000-year periodicity. When deep convection slowed in the North Atlantic, the North Atlantic region cooled. When deep convection slowed near Antarctica, Antarctica cooled.

a) Provide a physical explanation for how surface temperatures cooled when the formation of deep water slowed.

b) These millennial oscillations persisted throughout the Holocene, but at significantly smaller amplitude relative to during the last ice age. What physical aspect of the globe was quite different during the Holocene and how could it affect the amplitude of the millennial oscillation?

c) It appears that anthropogenic greenhouse warming is causing serious reduction in the volume of Arctic sea ice and may be starting to cause significant melting of Greenland. In light of the above physical processes, describe what you think the temperature changes in the extratropical North Atlantic region would be under a global warming scenario.

References Cited

Alley, R. B., 2004: GISP2 Ice Core Temperature and Accumulation Data. IGBP PAGES / World Data Center for Paleoclimatology Data Contribution Series #2004-013. NOAA / NGDC Paleoclimatology Program, Boulder CO, USA.

Alley, R. B., 2000: The Younger Dryas cold interval as viewed from central Greenland. *Quat. Sci. Revs.*, **19**, 213-226.

Alley, R. B., et al., 1993: Abrupt increase in Greenland snow accumulation at the end of the Younger Dryas event. *Nature*, **362**, 527-529.

Ammann, C.M., G.A. Meehl, W.M. Washington, and C. S. Zender, 2003: A monthly and latitudinally varying volcanic forcing dataset in simulations of 20th century climate. *Geophys. Res. Letts.*, **30**, 1657-1660.

Broecker, W. S., 1992: in *The Last Deglaciation: Absolute and Radiocarbon Chronologies*, NATO ASI Series I, Vol. 2, Eds. E. Bard and W. S. Broecker, Springer-Verlag, Berlin, pp. 69-80.

Bryson, R.A., 1988: Late Quaternary Volcanic Modulation of Milankovitch Climate Forcing. *J. Theor. and Appl. Climatol.*, **39**, 115125.

Briffa, K. R., P. D. Jones, F. H. Schweingruber, and T. J. Osborn, 1998: Influence of volcanic eruptions on Northern Hemisphere summer temperature over the past 600 years. *Nature*, **393**, 450-454.

Baldwin, M. J., and T. J. Dunkerton, 2001: Stratospheric harbingers of anomalous weather regimes. *Science*, **294**, 581 - 584.

Barker, S., P. Diz, M. J. Vauitravers, J. Pike, G. Knorr, I. R. Hall, and W. S. Broecker, 2009: Interhemispheric Atlantic seesaw response during the last deglaciation. *Nature*, **457**, 1097-1102.

Broecker, W. S., 1998: Paleocean circulation during the last deglaciation: A bipolar seesaw? *Paleocean.*, **13**, 119-121.

Bryson, R. A., and R. U. Bryson, 1997: High resolution simulations of regional Holocene climate: North Africa and the Near East. In *Third Millenium BC Climate Change and*

Old World Collapse, Ed. H. N. Dalfes, G. Kukla and H. Weiss, pp. 565-593, vol. I 49. NATO ASI Series, Berlin.

Buhner, S. H., 1996: *Sacred Plant Medicine*, Roberts Rinehart Publs., Boulder, CO, 210 pp.

Bunker, A. F., 1976: Computations of surface energy flux and annual air-sea interaction cycles of the North Atlantic Ocean. *Mon. Wea. Rev.*, **104**, 1122-1140.

Cook, E. R., 2000: Southwestern USA Drought Index Reconstruction. International Tree-Ring Data Bank. IGBP PAGES / World Data Center for Paleoclimatology Data Contribution Series #2000-053. NOAA / NGDC Paleoclimatology Program, Boulder CO, USA.

Dansgaard, W., et al., 1982: A new Greenland deep ice core. *Science*, **218**, 1273-1277.

de Silva, S. L., and G. A. Zielinski, 1998: Global influence of the AD1600 eruption of Huaynaputina, Peru. *Nature*, **393**, 455-458.

Diamond, J., 2005: *Collapse: How Societies Choose to Fail or Succeed*, Penguin Books, New York, 592 pp.

EPICA Community Members, 2006: One-to-one coupling of glacial climate variability in Greenland and Antarctica. *Nature*, **444**, 195-198.

Hitchman, M. H., M. McKay, and C. R. Trepte, 1994: A climatology of stratospheric aerosol. *J. Geophys. Res.*, **99**, 20,689-20,700.

Gleick, J., 1987: *Chaos Theory*, Penguin Books, New York, NY, 352 pp.

Goodman, B., 1980: *Climatic impact of volcanic activity*, Ph.D. dissertation, Dept. of Meteorology, Univ. of Wisconsin-Madison.

Gupta, A. K., D. M. Anderson, and J. T. Overpeck, 2003: Abrupt changes in the Asian southwest monsoon during the Holocene and their links to the North Atlantic Ocean. *Nature*, **421**, 354-357.

Langford, A. O., T. J. O'Leary, M. H. Proffitt, and M. H. Hitchman, 1994: Transport of the Pinatubo Volcanic Aerosol to a Northern Midlatitude Site. *J. Geophys. Res.*, **100**, 9007-9016.

Lewis, C. F. M., et al., 2008: Dry climate disconnected the Laurentian Great Lakes. *EOS Trans.*, **89**, 541-542.

Miao, X., et al., 2007: A 10,000-year record of dune activity, dust storms, and severe drought in the central Great Plains. *Geology*, **35**, 119-122.

Miller, K. G., et al., 2009: The Phanerozoic record of global sea level change. *Science*, **310**, 1293-1298.

Oppenheimer, C., Climatic, environmental and human consequences of the largest known historic eruption: Tambora volcano (Indonesia) 1815. *Prog. Phys. Geog.*, **27**, 230-259.

Parker, G., 2008: “Crisis and Catastrophe: The Global Crisis of the 17th Century Reconsidered”, in *American Historical Review*, October.

Petit, J. R., et al., 1999: Climate and atmospheric history of the past 420,000 years from the Vostok ice core, Antarctica. *Nature*, **399**, 429-436.

Pickarski, N., O. Kwiecien, D. Langgut, and T. Litt, 2015: Abrupt climate and vegetation variability of eastern Anatolia during the last glacial. *Clim. Past.*, **11**, 1491–1505.

Pritz, K., 1991: *Westward Before Columbus*. Norsk Maritimt Forlag A/S, Oslo, Norway, 237 pp.

Reed, R. J., W. J. Campbell, J. A. Rasmussen, and R. G. Rogers, 1961: Evidence of a downward-propagating annual wind reversal in the equatorial stratosphere. *J. Geophys. Res.*, **66**, 613-618.

Rein, B., et al., 2005: El Nino variability off Peru during the last 20,000 years. *Paleoceanography*, **20**, PA4003.

Robock, A. 2000. Volcanic eruptions and climate. *Rev. Geophys.*, **38**, 191-219.

Ruddiman, W. F., 2003: The anthropogenic greenhouse era began thousands of years ago. *Clim. Change*, **61**, 261-293.

Ruddiman, W. F., 2007: The early anthropogenic hypothesis: Challenges and responses. *Rev. Geophys.*, **45**, RG4001.

Ryan, W.B., and W.C. Pitman, 1998: Noah's Flood: The new scientific discoveries about the event that changed history. Simon and Schuster, New York, 319 pp.

Sato, Mki., J.E. Hansen, M.P. McCormick, and J.B. Pollack, 1993: Stratospheric aerosol optical depths, 1850-1990. *J. Geophys. Res.*, **98**, 22987-22994

Sabine, C. L., et al., 2004: The oceanic sink for anthropogenic CO_2. *Science*, **305**, 367-371.

Thompson, D.W.J., and J.M. Wallace, 2001: Regional climate impacts of the Northern Hemisphere annular mode. *Science*, **293**, 85-89.

Trepte, C. R., R. E. Veiga, and M. P. McCormick, 1993: The poleward dispersal of Mount Pinatubo volcanic aerosol. *J. Geophys. Res.*, **98**, 18,563-18,573.

Weaver, A. J., O. A. Saenko, P. U. Clark, and J. X. Mitrovica, 2003: Meltwater pulse 1A from Antarctica as a trigger of the Bolling-Allerod warm interval. *Science*, **299**, 1709-1713.

Winchester, S., 2002: *Krakatoa: The Day the World Exploded, August 27, 1883*, Harper Collings, 448 pp.

Zielinski, G.A., and G.R. Mershon, 1997: Paleoenvironmental implications of the insoluble microparticle record in the GISP2 (Greenland) ice core during the rapidly changing climate of the Pleistocene-Holocene transition. *Bull. Geol. Soc. Amer.*, **109**, 547-559.